Nature Communications

https://doi.org/10.1038/s41467-026-68963-7

Article in Press

Synthesis of poly(ester disulfide)s from S_8-involved step-growth addition polymerization at ambient temperature

Received: 1 September 2025

Accepted: 19 January 2026

Cite this article as: Sun, Y., Cao, Y., Liu, X. *et al.* Synthesis of poly(ester disulfide)s from S_8-involved step-growth addition polymerization at ambient temperature. *Nat Commun* (2026). https://doi.org/10.1038/s41467-026-68963-7

Yue Sun, Yuxiang Cao, Xiong Liu, Chengjian Zhang & Xinghong Zhang

Synthesis of poly(ester disulfide)s from S_8-involved step-growth addition polymerization at ambient temperature

Yue Sun,[1,2,3] Yuxiang Cao,[1,2] Xiong Liu,[1,2] Chengjian Zhang,[1,2]* and Xinghong Zhang[1,2]

[1]State Key Laboratory of Biobased Transportation Fuel Technology, International Research Center for X Polymers, Department of Polymer Science and Engineering, Zhejiang University, Hangzhou 310027 (China)

[2]Zhejiang Key Laboratory of Low-Carbon Synthesis of Value-Added Chemicals, Department of Chemistry, Zhejiang University, Hangzhou 310027 (China)

[3]National Engineering Research Center of Coal Gasification and Coal-Based Advanced Materials, Shandong Energy Group Coal Gasification New Material Technology Co. LTD, Jinan 250220 (China)

Corresponding author (*): chengjian.zhang@zju.edu.cn (Chengjian Zhang)

Abstract

Elemental sulfur (S_8), an abundant petroleum byproduct, is leveraged as a linchpin monomer in an organobase-catalyzed step-growth addition polymerization with dithiols and diacrylates at ambient temperature. This method enables the scalable synthesis of poly(ester disulfide)s—featuring alternating ester and disulfide linkages—with exceptional atom economy (>95% yield), M_n up to 42.0 kDa, and dual functionality: biodegradable ester units and stimuli-responsive disulfides. Mechanistic studies reveal a chemoselective three-component coupling involving S_8 ring-opening, disulfide anion formation, and Michael addition, quantitatively generating symmetric and asymmetric disulfides in near-equimolar ratios. Thermal and mechanical characterizations of the poly(ester disulfide)s reveal programmable properties: High thermal stability ($T_{d,5\%}$ = 248–281 °C), tunable phase behavior (amorphous T_g = −64 °C to semicrystalline T_m = 142 °C), and reductive degradation. By overcoming traditional limitations of harsh conditions and monomer scope, this strategy establishes S_8 as a versatile feedstock for functional polymers, opening avenues for dynamic materials in biomedicine and environmental remediation.

Introduction

Synthetic polymers featuring dynamic covalent backbones have emerged as transformative materials in fields ranging from recyclable plastics to adaptive biomaterials.[1-3] Poly(disulfide)s—characterized by sulfur-sulfur (S–S) linkages within their backbone—have attracted significant interest due to their unique redox-responsive behavior, self-healing capabilities, and potential for degradation.[4-8] The disulfide bond, a cornerstone of dynamic chemistry, undergoes reversible cleavage and reformation under mild stimuli (e.g., light, redox agents, or mechanical force), enabling applications in drug delivery, smart coatings, and energy storage.[9-15] However, conventional synthetic routes to poly(disulfide)s face critical challenges.[16-22]

Traditional approaches to poly(disulfide)s rely on oxidative coupling of dithiols or ring-opening polymerization (ROP) of cyclic disulfides (Figure 1a).[23-28] The oxidative coupling of dithiols often suffers from competing side reactions (e.g., overoxidation to sulfonic acids) and kinetic trapping of intermediates, resulting in low-molecular-weight polymers.[29] Although ROP offers enhanced control, the synthesis of strained cyclic disulfide monomers typically requires multistep routes with harsh conditions, limiting structure/property diversity of poly(disulfide)s. Recent advances, such as the polycondensation of disulfide-containing monomers,[29] have improved efficiency, yet scalability and narrow monomer scope remain persistent hurdles. Notably, Pyun, Njardarson, Norwood, and coworkers reported the step-growth addition polymerization of sulfur monochloride with allylic monomers, affording highly optically transparent disulfide-containing thermosets.[30] Against this backdrop, the development of mild, atom-economical, and

robust synthetic methods for poly(disulfide)s remains a critical unmet need.

Elemental sulfur (S_8), an abundant byproduct of petroleum refining (80 million tons/year), represents an ideal, low-cost feedstock for polymer synthesis.[31,32] Despite this potential, S_8 remains underutilized in macromolecular science due to challenges of its ring-strain-driven polymerization.[33,34] Initial breakthroughs, such as Pyun and co-workers' inverse vulcanization of S_8 with 1,3-diisopropenyl benzene (requiring 160 °C), yielded brittle and insoluble high-sulfur-content materials (Figure 1b).[35] Subsequent strategies expanded S_8's utility.[36-46] Hu, Tang, and co-workers achieved room-temperature synthesis of poly(thiourea)s via multi-component polymerization of S_8, aliphatic diamines, and diisocyanides.[47-49] Ren and co-workers developed the copolymerization of S_8 with episulfides to access poly(disulfide)s via an anionic chain-growth mechanism.[50] Nevertheless, the direct exploitation of S_8 in step-growth polymerization to poly(disulfide)s remains largely unexplored. Building on this foundation, we envisioned S_8 as a key monomer in step-growth polymerization to precisely synthesize poly(ester disulfide)s—a polymer integrating the biodegradability of esters with the dynamic responsiveness of disulfides.

Herein, we report the synthesis of poly(ester disulfide)s via an organobase-catalyzed step-growth addition polymerization of S_8, dithiols, and diacrylates at room temperature (Figure 1c). This methodology capitalizes on S_8 inherent reactivity with diacrylates, enabling the formation of alternating ester and disulfide linkages under mild conditions. The polymerization proceeds efficiently with excellent atom economy and scalability, yielding polymers with tunable thermal/mechanical properties and multi-stimuli-responsive degradation behavior. Beyond expanding the scope of S_8-based polymerizations, this work establishes a platform for functional

poly(disulfide)s by integrating elemental sulfur into step-growth polymerizations. The operational simplicity and versatility of this approach offer convenient pathways to engineer dynamic, biodegradable polymers for biomedical and environmental applications.

Results

We first established a model reaction using S_8, 1-hexanethiol, and methyl acrylate (MA) as reactants (Figure 2a). Common organic bases[51]—including 7-methyl-1,5,7-triazabicyclo[4.4.0]dec-5-ene (MTBD), 4-dimethylaminopyridine (DMAP), tetrabutylammonium acetate, and 1,4-diazabicyclo[2.2.2]octane (DABCO)—exhibited high activity and selectivity in this three-component coupling. Due to S_8's limited solubility, we adopted a sequential addition protocol: S_8 and MTBD were pre-mixed in solvent to achieve dissolution, followed by addition of 1-hexanethiol and MA. Under optimized conditions, ($[S\ atoms]_0$:$[thiol\ groups]_0$:$[MA]_0$:[base] = 400:400:400:1, rt, 0.5 h) in toluene, acetonitrile, 1,4-dioxane, or acetone, the reaction quantitatively generated three disulfide products (**A1–A3**). The complete reactant conversion was confirmed by ^{1}H and ^{13}C NMR analysis of crude products (Figures 2b, 2c, S1, and S2).

The mixed disulfide products (**A1–A3**) were separated by column chromatography. Symmetrical **A3** was first isolated using *n*-hexane as an eluent, followed by the separation of **A1** and **A2** with *n*-hexane:dichloromethane = 2:3 (v/v). After drying in vacuo to constant weight, pure **A1**–**A3** were obtained in 95% combined yield, with a gravimetrically determined molar ratio of [**A1**]:[**A2**]:[**A3**] = 1.00:1.02:0.98. Structures of **A1**–**A3** were confirmed by ^{1}H and ^{13}C NMR

(Figures 2d, 2e, S3–S8) and ESI–MS.

Notably, the ^{1}H NMR spectrum of **A1** closely matched the corresponding signals in the crude mixture **A1–A3** (Figure 2f), indicating minimal electronic coupling across the disulfide bond. While ^{13}C NMR peaks for **A2**/**A3** were distinct from **A1**, key resonances exhibited similarity (e.g., **A2**-b at 172.35 ppm vs. **A1**-b' at 172.17 ppm; Figure 2g). The integration of crude product ^{13}C NMR spectrum confirmed the molar ratio of [**A1**]:[**A2**]:[**A3**] = 1.00:1.08:1.04. Critically, the NMR analysis detected no by-products (e.g., thiol-MA adducts,[52] sulfur-MA copolymers,[53] or polysulfides[54]), demonstrating an exceptional chemoselectivity in the organobase-catalyzed three-component coupling reaction. Kinetic analysis via ^{1}H NMR (Figures S9 and S10) confirmed the exclusive formation of disulfide products from the earliest observable reaction stage, inconsistent with a plausible mechanism proceeding through a kinetic distribution of polysulfide intermediates.

We extended this methodology to additional substrates, including the enone (1-octene-3-one), *N*-(methoxymethyl)acrylamide, and other thiols (1-octanethiol, benzyl mercaptan). Under identical mild conditions ($[\text{S atoms}]_0$:$[\text{thiol groups}]_0$:$[\text{alkene groups}]_0$:[MTBD] = 400:400:400:1, rt, 0.5 h, toluene), these reactions quantitatively generated three mixed disulfide products in a near-equimolar ratio, which is similar to the production of **A1–A3**. The column chromatography method afforded all distinct disulfides—including asymmetric variants—in high purity with >95% combined yields (Figures S11–S32). While used here for efficient product isolation on an analytical scale, future work will focus on developing sustainable work-up procedures, such as precipitation or catalysis in greener solvent systems, for larger-scale applications. Notably, the synthesis of asymmetric disulfides confronts persistent challenges: (1) thermodynamic preference

for symmetric disulfides via thiol-disulfide exchange, (2) inherent chemoselectivity limitations in direct coupling, (3) instability of sulfenyl halide intermediates, and (4) arduous separation from symmetric byproducts.[55-60] Our method establishes a mild and modular route to asymmetric disulfides containing other functional groups such as ester, amide, and ketone.

We then performed density functional theory (DFT) calculations to elucidate the three-component coupling mechanism. The DFT calculations employed small-molecule analogues to model the key mechanistic steps of the polymerization. The calculated details were shown in Supplementary Information (Figures S64–S68). The free energy profile (Figure 3a) reveals the initiation via the MTBD-mediated deprotonation of thiol to form a thiolate anion (**S1**). The subsequent nucleophilic attack on S_8 ring-opens the cyclooctasulfur to generate a linear polysulfide anion (**S2**). The chain-shortening through an intramolecular substitution (**TS2**) then yields a disulfide anion (**S3**) and S_7. The Michael addition of **S3** to methyl acrylate (**TS3**), followed by a protonation, affords the asymmetric disulfide of **S5**. Crucially, the thiol-disulfide exchange reaction between **S5** and thiolate (**TS4/TS5**) proceeds with low energy barriers ($\Delta G^{\ddagger}$ = 5.0–6.0 kcal mol^{-1}), equilibrating the symmetric disulfides of **S6** and **S7** (Figures 3b and 3c). The near-isoenergetic nature of **S5–S7** ($\Delta G \leq 6.4$ kcal mol^{-1}) thermodynamically favors the near-equimolar product distribution—validating the experimental observations.

We next applied this methodology to synthesize poly(ester disulfide)s using commercially available bifunctional monomers. The used dithiol monomers comprised 1,6-hexanedithiol, 1,8-octanedithiol, 1,10-decanedithiol, and *p*-benzyldithiol; the used diacrylates included 1,6-hexanediol diacrylate, 1,9-nonanediol diacrylate, and 1,10-decanediol diacrylate (Figure 4). The

multicomponent step-growth addition polymerization of S_8, 1,6-hexanedithiol, and 1,6-hexanediol diacrylate ([S atoms]$_0$:[thiol groups]$_0$:[alkene groups]$_0$:[MTBD] = 400:400:400:1, rt, 2 h) afforded **P1** in 97% yield (by gravimetry) with M_n = 10.2 kDa as determined by gel permeation chromatography (GPC, calibrated with polystyrene standards). Notably, the addition of bis(triphenylphosphine)iminium chloride ([PPN]Cl) to the polymerization system as a cocatalyst enhanced the molecular weight of the polymer. Using a fixed MTBD loading (0.25 mol%) while varying the amount of [PPN]Cl, the results presented in Table S1 demonstrate a clear dose-dependent effect of [PPN]Cl on the reaction outcome. Upon addition of [PPN]Cl, the molecular weight increased progressively with the co-catalyst loading, plateauing at an M_n of 22.1 kDa ($Đ$ = 2.3) when using a 1:1 molar ratio of [PPN]Cl to MTBD. To test the specificity of the PPN^+ cation and rule out a simple ionic strength effect, we performed the polymerization using MTBD with equivalent molar amounts of other salts including tetrabutylammonium chloride (NBu_4Cl) and bis(triphenylphosphine)iminium trifluoroacetate ([PPN]TFA). The results included in Table S1 show that while NBu_4Cl provided a modest increase in M_n to 12.5 kDa, it was significantly less effective than PPNCl. Similar to [PPN]Cl, [PPN]TFA showed a high effect increase in M_n to 20.9 kDa. This comparison indicates that the PPN^+ cation plays a specific and crucial role. We propose that the large, highly lipophilic PPN^+ cation acts as an effective phase-transfer catalyst, solubilizing the anionic sulfur intermediates and enhancing their reactivity in the organic reaction medium, which is consistent with the reported mechanism in S_8 and episulfide copolymerization.[50]

Similarly, under identical conditions ([S atoms]$_0$:[thiol groups]$_0$:[alkene groups]$_0$:[MTBD] = 400:400:400:1, rt, 2 h), **P2–P6** were synthesized in >95% yields with M_n = 20.8–42.0 kDa ($Đ$ =

1.4–2.6, as determined by GPC calibrated with polystyrene standards, Figure S43), indicating the facile and versatile manners of the synthetic method. According to the GPC test equipped with a multiangle light scattering detector (GPC-MALS, Figure S44), **P1–P6** possessed absolute M_n of 28.4 kDa ($Đ$ = 1.9), 23.6 kDa ($Đ$ = 1.3), 24.3 kDa ($Đ$ = 1.4), 51.4 kDa ($Đ$ = 2.6), and 34.7 kDa ($Đ$ = 2.6), respectively. The absolute M_n values are slightly higher than the relative M_n values as determined by GPC. The molecular weights achieved in this work are characteristic of the step-growth mechanism, where high molecular weights require extreme conversion. The values obtained are a consequence of the mild reaction conditions, which were prioritized to enable functional group tolerance and precise sequence control over the disulfide and ester linkages. Additionally, the identification of a cheaper, more sustainable organocatalyst with comparable activity is a target for future scale-up and process optimization. We also calculated the *E*-factor (kg waste/kg product)[61] for the synthesis of polymers **P1-P6**, including all reactants, solvents, and purification steps. The calculated *E*-factor values are around 20, in which ethanol used in the purification step is the major contributing waste to the *E*-factor. This value falls in the range of the *E*-factor demanded by fine chemical industries (5–50), and is higher than that of the reported inverse vulcanization (0.1–5).[61]

The obtained polymers (**P1–P6**) feature both S–S and ester linkages within their backbone, as confirmed by NMR analysis (Figures 5a, 5b, S33–S42). Notably, the ^{13}C NMR spectra (Figure 5b) exhibit the characteristic peak doublets of near-equal integration—mirroring small-molecule disulfide patterns—quantitatively validating a near 1:1:1 molar ratio of three disulfide units in the polymer chain. The Raman spectroscopy of the poly(ester disulfide)s further corroborated their

backbone structures through the distinct ν(S-S) and ν(C-S) vibrations. The Raman spectrum (Figure 5c) shows a single peak at 510 cm^{-1}, which aligns perfectly with the disulfide standard and is distinctly different from the S_8 peak (~470 cm^{-1})[62] and the polysulfide peak (~540 cm^{-1}).[36,50] Critically, the MALDI-TOF mass spectrometry of **P1** unambiguously confirmed the disulfide repeat units and revealed the comparable incorporation of symmetric/asymmetric motifs ($n \approx m$, Figure 5d) in the polymer backbone. Additionally, the elemental analysis result of **P1** (C, 48.7%; N, 0%; S, 29.4%; H, 6.9%) closely matched the theoretical values, e.g., C, 49.1%; N, 0%; S, 29.1%; H, 7.3%. This confirms the bulk stoichiometry and rules out significant contamination from unreacted S_8 or large deviations in composition. Furthermore, the high-resolution X-ray photoelectron spectroscopy (XPS) *S 2p* spectrum (Figure S45) displays 1:2 integral area ratio of the XPS peaks representing S-S and C-S bonds, suggesting the presence of most of disulfide units.[50] No significant peaks near 161-162 eV are observed, which would suggest the presence of unreacted S_8 or sulfide anions. This provides direct chemical state evidence for the exclusive presence of disulfide linkages in the near-surface region of the polymer.

The thermal and mechanical characterizations reveal the distinct structure-property relationships in polymers **P1** to **P6**. The thermogravimetric analysis (TGA, Figure 6a) demonstrates moderate thermal stability for all polymers, with decomposition temperatures ($T_{d,5\%}$) ranging from 248 °C to 281 °C (Table S2). The differential scanning calorimetry (DSC, Figure 6b) shows that **P1** and **P2** are amorphous materials exhibiting remarkably low glass transition temperatures (T_g) of -60 °C and -64 °C, respectively. In contrast, **P3** and **P4** display semi-crystalline behaviors, characterized by melting temperatures (T_m) of 27 °C and 30 °C, attributed

to the presence of long carbon chains (10 carbon atoms) in the polymer backbone. Incorporating rigid benzene rings into the main chain (**P5**) significantly enhances crystallinity of the polymer, yielding a high T_m of 142 °C (Figure 6b). Additionally, the absence of any endothermic peak at ~119 °C (which S_8 melts) across all first-heating scans (Figures S46-S51) provides strong evidence for the complete consumption and clean incorporation of S_8, ruling out its presence as a crystalline contaminant.

The tensile stress-strain measurements (Fig. 6c) identify **P4** and **P5** as thermoplastic elastomers (TPEs). **P4** exhibits an ultimate tensile strength (σ_B) of 0.21 ± 0.06 MPa and an exceptional elongation at break (ε_B) of 2320 ± 590% (Figure S52). **P5** possesses a higher σ_B of 1.0 ± 0.1 MPa but a reduced ε_B of 840 ± 63% (Figure S53). The cyclic tensile testing further confirmed their elastomeric nature: samples were stretched to 50% (**P5**) or 100% (**P4**) strain and immediately released to 0% strain at 10 mm min^{-1} for 10 consecutive cycles (Figs. 6d and 6e). Both polymers exhibited high elastic recovery, with calculated recovery rates [(ε_{max} - $\varepsilon_{residual}$) / ε_{max}] of 91% (**P5**) and 74% (**P4**) maintained over ten cycles without significant fatigue. The hysteresis energy and the residual strain (Table S3) of **P4** and **P5** remained relatively consistent and stable after the first cycle, characteristic of a robust elastomeric network. This mechanical performance is comparable to that of the high-molecular-weight (over 1000 kDa) poly(1,2-dithiolane) (σ_B of ~0.5 MPa and ε_B of ~500%) synthesized from the ROP of 1,2-dithiolanes in the previous study.[20] **P6**, featuring in-chain amide groups that enable hydrogen bonding, adopts a crystalline structure with a T_m of 119 °C (Figure 6b). This network of secondary interactions enhances mechanical strength, resulting in a higher σ_B of 4.0 ± 1.7 MPa, though it reduces ductility (ε_B = 92 ± 14%, Figures 6c

and S54) compared to the elastomeric analogues. Notably, the range of accessible structures and properties for these polymers can be greatly expanded by the versatility of our method and the broad scope of compatible monomers.

A defining characteristic of disulfide bonds is their susceptibility to reductive cleavage. **P2** was used as a representative polymer for the degradation experiment because **P1** to **P6** possesses similar functional groups and structures. To demonstrate this responsiveness in our system, **P2** was subjected to reductive degradation using DL-dithiothreitol (DTT) as the reducing agent. The depolymerization kinetics were monitored in real-time by periodically sampling the reaction mixture and analyzing molecular weight evolution via GPC. As shown in Figure 6f, the polymer cleavage commenced immediately upon DTT addition, triggering a rapid decrease in molecular weight of the polymer. Within 1 hour, a significant shift towards lower molecular weights was observed (M_n decreased from 20.8 to 8.1 kDa). The degradation progressed continuously over the 20-hour reaction period (Figure S55), ultimately converting the majority of the polymer into oligomeric species, indicating the rapid and quantitatively reductive degradability of the polymeric materials. The primary degradation products are the small-molecule dithiol and the Michael addition adduct (the monomeric units), as determined by ^{1}H NMR (Figure S56) and gas chromatography quadrupole-time of flight mass spectrometry (Figure S57). Other common effective reductants such as tris(2-carboxyethyl)phosphine and glutathione would be more relevant for biomedical or environmental claims in practical applications. Additionally, the polymers proved stable for three months when stored in air at room temperature, with no detectable changes in their properties, indicating sufficient robustness for practical handling and applications. Future

studies will explore orthogonal degradation cascades, such as the selective hydrolysis of ester linkages under mild basic conditions to fragment the polymer backbone while preserving the disulfide dynamic units, enabling sophisticated, multi-stage degradation profiles.

We further demonstrated that the disulfide linkages in both the small-molecule model **A1** and polymer **P3** can undergo a base-catalyzed sulfur insertion reaction with additional S_8, effectively incorporating more sulfur atoms into the structure.[63] Under optimized conditions ([**A1**]$_0$:[MTBD] = 400:1, rt, 0.5 h, toluene), increasing the S_8 feed ratio from [S atoms]$_0$:[**A1**]$_0$ = 0.5 to 2 led to a dose-dependent increase in polysulfide product formation, accompanied by a corresponding decrease in **A1**, as monitored by ^{1}H NMR (Figure S58). A similar trend was observed for polymer **P3**: as the S_8 loading increased from [S atoms]$_0$:[disulfide units]$_0$ = 1 to 3, the resulting polymers **P3′** and **P3″** exhibited progressively higher polysulfide content and reduced disulfide unit ratios (Figure S59). Concomitantly, the M_n values decreased from 21.3 kDa for **P3** to 8.8 kDa for **P3′** and 5.3 kDa for **P3″** (Figure S60). Thermal analysis revealed that the incorporation of less-stable polysulfide linkages also lowered the decomposition temperatures ($T_{d,5\%}$: 281 °C for **P3**, 241 °C for **P3′**, and 208 °C for **P3″**; Figure S61) and suppressed melting transitions, while slightly raising the T_g values (−65 °C for **P3**, −64 °C for **P3′**, −62 °C for **P3″**; Figures S62 and S63).

In conclusion, this work establishes elemental sulfur as a cornerstone monomer for synthesizing functional poly(ester disulfide)s through an organobase-catalyzed step-growth polymerization at ambient temperature. By leveraging the inherent reactivity of S_8 with commercially available dithiols and diacrylates, we achieve alternating ester and disulfide linkages in high yields (>95%) with M_n up to 42.0 kDa. Mechanistic studies, supported by DFT calculations,

confirm a chemoselective three-component pathway that quantitatively generates near-equimolar symmetric and asymmetric disulfide units—validated by MALDI-TOF, NMR, and Raman spectroscopy. Critically, backbone engineering enables precise control over material properties: Long aliphatic chains yield thermoplastic elastomers with exceptional elasticity, while rigid aromatic or hydrogen-bonding units enhance strength. The poly(ester disulfide)s exhibit high thermal stability and rapid reductive degradation to oligomers, underscoring their circular lifecycle. Collectively, this strategy transforms an industrial byproduct (80 million tons/year) into a versatile platform for advanced materials. The fusion of dynamic responsiveness, engineered mechanical performance, and reductive degradability opens avenues for adaptive biomaterials, elastomers, and coatings. Furthermore, the potential to exploit differential monomer reactivity to synthesize sequence-defined and block copolymers represents a compelling direction for future research.

Methods

Materials

Elemental sulfur (99.5%), toluene (99.5%), and acetone (99.5%) were purchased from Sinopharm Chemical Reagent Co., Ltd. 1-Hexanethiol (96%), 1-octen-3-one (97%), 1,6-hexanedithiol (98%), 1,10-decanedithiol (98%), 1,8-octanedithiol (97.5%), 1,4-dioxane (99.5%, super dry solvent), acetonitrile (MeCN, 99.9%, super dry solvent), benzyl mercaptan (99%), PPNCl (97%), DABCO (97%), DMAP (99%), and tetrabutylammonium acetate (93%) were obtained from J&K Scientific Ltd. 1-Octanethiol (98%) was supplied by Tokyo Chemical Industry Co., Ltd. MTBD (95%) was acquired from Aladdin Biochemical Technology Co., Ltd.

Characterization and processing techniques

^{1}H and ^{13}C NMR spectra were performed on a Bruker Advance DMX 400 MHz. And chemical

shift values were referenced to the signal of the solvent (residual proton resonances for ^{1}H NMR spectra, carbon resonances for ^{13}C NMR spectra).

M_n and $Đ$ of the polymers were measured by GPC at 40°C using a PL-GPC220 chromatograph equipped with an Agilent Technologies HP 1100 pump. The measurement was performed with THF as the mobile phase at a flow rate of 1.0 mL/min. The sample concentration was 0.4 wt.%, and the injection volume was 50 μL. Calibration was performed using monodisperse polystyrene standards.

The absolute M_n values of the polymers were performed by GPC equipped with multiangle light scattering detector. Light scattering, viscosity and RI were determined by DAWN, ViscoStar and Optilab from Wyatt, respectively. The refractive index increment (dn/dc) values of **P1** to **P5** obtained by batch experiments using Optilab from Wyatt and calculated using ASTRA software.

MALDI-TOF MS was performed on a Bruker Ultraflex MALDI-TOF mass spectrometer equipped with a nitrogen laser emitting 337 nm laser pulses (3 ns pulse width). *Trans*-2-[3-(4-*tert*-butylphenyl)-2-methyl-2-propenylidene]malononitrile was used as the matrix, with sodium trifluoroacetate added to enhance ionization.

ESI-MS was performed using an Agilent G6545 mass spectrometer. The sample was dissolved in THF at a concentration of 1 mg/mL for analysis.

T_d values of the polymers were determined by using TA Q50 instrument. The sample was heated from 40 to 600 °C at a rate of 10 °C/min under nitrogen atmosphere. Temperature when the mass loss is five percent was taken as $T_{d,5\%}$.

DSC measurements of polymers were carried out on a TA Q200 instrument with a heating/cooling rate of 10 °C/min. Data reported are from second heating cycles.

Tensile tests were performed on an Instron 3343 instrument at a crosshead speed of 20

mm/min on compression-moulded tensile testing specimens.

Elemental analysis was conducted at the equipment of Arvato CRM China EA3000 (CHNS).

Raman spectra were recorded on a Renishaw plc inVia-Reflex equipped with a low-temperature Ge detector (532 nm, 50 mW, resolution 2 cm^{-1}, 30 seconds per accumulation, 5 accumulations). Peaks were assigned based on comparison with literature values for disulfide and polysulfide vibrations.

XPS was measured on Thermo ESCALAB XI^{+}. A monochromatic Al K_{α} X^{-} ray source was used, with the energy of 1486.6 eV. Charge compensation was needed.

GC/Q-TOF MS was performed on Agilent 7250 GC/Q-TOF (Mode of ionizations: Electron ionization, low energy electron ionization; Mass range: 20-3000 amu; Mass analyzer 1: Quadrupole; Collision cell: Hexapole; Mass analyzer 2: Time-of-flight; Detector: Photomultiplier tube).

Reductive degradation experiment

P2 was subjected to reductive degradation using DTT as the reducing agent. To a solution of 30 mg of the polymer in 2 mL of THF was added 115 mg of DTT. The molecular weight change was monitored by GPC analysis of 100 μL aliquots withdrawn from the reaction mixture at designated intervals.

Data availability

Data supporting the findings of this study are available within the article (and its Supplementary information files). All data are available from the corresponding author upon request.

References

(1) Zheng, N.; Xu, Y.; Zhao, Q.; Xie, T. Dynamic Covalent Polymer Networks: A Molecular Platform for Designing Functions beyond Chemical Recycling and Self-Healing. *Chemical Reviews* **2021**, *121*, 1716-1745.

(2) Lei, Z.; Chen, H.; Huang, S.; Wayment, L. J.; Xu, Q.; Zhang, W. New Advances in Covalent Network Polymers via Dynamic Covalent Chemistry. *Chemical Reviews* **2024**, *124*, 7829-7906.

(3) Maes, S.; Badi, N.; Winne, J. M.; Du Prez, F. E. Taking dynamic covalent chemistry out of the lab and into reprocessable industrial thermosets. *Nature Reviews Chemistry* **2025**, *9*, 144-158.

(4) Pal, S.; Shin, J.; DeFrates, K.; Arslan, M.; Dale, K.; Chen, H.; Ramirez, D.; Messersmith, P. B. Recyclable surgical, consumer, and industrial adhesives of poly(α-lipoic acid). *Science* **2024**, *385*, 877-883.

(5) Zhang, Q.; Qu, D.-H.; Feringa, B. L.; Tian, H. Disulfide-Mediated Reversible Polymerization toward Intrinsically Dynamic Smart Materials. *Journal of the American Chemical Society* **2022**, *144*, 2022-2033.

(6) Deng, Y.; Zhang, Q.; Shi, C.; Toyoda, R.; Qu, D.-H.; Tian, H.; Feringa, B. L. Acylhydrazine-based reticular hydrogen bonds enable robust, tough, and dynamic supramolecular materials. *Science Advances* **2022**, *8*, eabk3286.

(7) Bang, E.-K.; Lista, M.; Sforazzini, G.; Sakai, N.; Matile, S. Poly(disulfide)s. *Chemical Science* **2012**, *3*, 1752-1763.

(8) Mutlu, H.; Ceper, E. B.; Li, X.; Yang, J.; Dong, W.; Ozmen, M. M.; Theato, P. Sulfur

Chemistry in Polymer and Materials Science. *Macromolecular Rapid Communications* **2019**, *40*, 1800650.

(9) Machado, T. O.; Stubbs, C. J.; Chiaradia, V.; Alraddadi, M. A.; Brandolese, A.; Worch, J. C.; Dove, A. P. A renewably sourced, circular photopolymer resin for additive manufacturing. *Nature* **2024**, *629*, 1069-1074.

(10) Zhang, X.; Waymouth, R. M. 1,2-Dithiolane-Derived Dynamic, Covalent Materials: Cooperative Self-Assembly and Reversible Cross-Linking. *Journal of the American Chemical Society* **2017**, *139*, 3822-3833.

(11) Lu, J.; Dai, Y.; He, Y.; Zhang, T.; Zhang, J.; Chen, X.; Jiang, C.; Lu, H. Organ/Cell-Selective Intracellular Delivery of Biologics via N-Acetylated Galactosamine-Functionalized Polydisulfide Conjugates. *Journal of the American Chemical Society* **2024**, *146*, 3974-3983.

(12) Guo, J.; Zhang, S.; Tao, Y.; Zheng, W.; Cheng, H.; Li, H.; Wang, Z.; Gou, Y.; Zhu, J.; Li, L.; Liu, Y.; Becker, M. L.; Tang, W. Synthesis of Cationic Cyclic Oligo(disulfide)s via Cyclo-Depolymerization: A Redox-Responsive and Potent Antibacterial Reagent. *Journal of the American Chemical Society* **2025**, *147*, 6772-6785.

(13) Yu, D.; Wang, Y.; Qu, S.; Zhang, N.; Nie, K.; Wang, J.; Huang, Y.; Sui, D.; Yu, B.; Qin, M.; Xu, F.-J. Controllable Star Cationic Poly(Disulfide)s Achieve Genetically Cascade Catalytic Therapy by Delivering Bifunctional Fusion Plasmids. *Advanced Materials* **2023**, *35*, 2307190.

(14) Huang, H.; Wang, H.; Sun, L.; Zhang, R.; Zhang, L.; Wu, Z.; Zheng, Y.; Wang, Y.; Fu, W.; Zhang, Y.; Neisiany, R. E.; You, Z. Long-Range Electronic Effect-Promoted Ring-Opening Polymerization of Thioctic Acid to Produce Biomimetic Ionic Elastomers for Bioelectronics. *CCS*

Chemistry **2024**, *6*, 761-773.

(15) Shi, C.-Y.; He, D.-D.; Zhang, Q.; Tong, F.; Shi, Z.-T.; Tian, H.; Qu, D.-H. Robust and dynamic underwater adhesives enabled by catechol-functionalized poly(disulfides) network. *National Science Review* **2023**, *10*, nwac139.

(16) Du, T.; Shen, B.; Dai, J.; Zhang, M.; Chen, X.; Yu, P.; Liu, Y. Controlled and Regioselective Ring-Opening Polymerization for Poly(disulfide)s by Anion-Binding Catalysis. *Journal of the American Chemical Society* **2023**, *145*, 27788-27799.

(17) Liu, Y.; Jia, Y.; Wu, Q.; Moore, J. S. Architecture-Controlled Ring-Opening Polymerization for Dynamic Covalent Poly(disulfide)s. *Journal of the American Chemical Society* **2019**, *141*, 17075-17080.

(18) Gallizioli, C.; Deglmann, P.; Plajer, A. J. Kinetically Enhanced Access to a Dynamic Polyester Platform via Sequence Selective Terpolymerisation of Elemental Sulphur. *Angewandte Chemie International Edition* **2025**, e202501337.

(19) Zhang, Q.; Deng, Y.-X.; Luo, H.-X.; Shi, C.-Y.; Geise, G. M.; Feringa, B. L.; Tian, H.; Qu, D.-H. Assembling a Natural Small Molecule into a Supramolecular Network with High Structural Order and Dynamic Functions. *Journal of the American Chemical Society* **2019**, *141*, 12804-12814.

(20) Wang, B.-S.; Zhang, Q.; Wang, Z.-Q.; Shi, C.-Y.; Gong, X.-Q.; Tian, H.; Qu, D.-H. Acid-catalyzed Disulfide-mediated Reversible Polymerization for Recyclable Dynamic Covalent Materials. *Angewandte Chemie International Edition* **2023**, *62*, e202215329.

(21) Albanese, K. R.; Morris, P. T.; Read de Alaniz, J.; Bates, C. M.; Hawker, C. J. Controlled-

Radical Polymerization of α-Lipoic Acid: A General Route to Degradable Vinyl Copolymers. *Journal of the American Chemical Society* **2023**, *145*, 22728-22734.

(22) Fang, J.; Ji, C.; Meng, Y.; Ye, P.; Zhang, H.; Li, W. Electrochemical Polymerization of 1,2-Dithiolane Derivatives at Room Temperature. *Angewandte Chemie International Edition* **2025**, e202506724.

(23) Kandemir, D.; Luleburgaz, S.; Gunay, U. S.; Durmaz, H.; Kumbaraci, V. Ultrafast Poly(disulfide) Synthesis in the Presence of Organocatalysts. *Macromolecules* **2022**, *55*, 7806-7816.

(24) Mu, Y.; Li, J.; Wang, J.; Ying, J.; Huang, C.; Zhou, X.; Zhou, T.; Liu, X.; Shen, Y.; Zhou, Q. Polymerization-Induced Self-Coacervation of Alternating Poly(disulfide)s via Ring-Opening Reaction-Mediated Polycondensation of Cyclic Thiosulfinate and Dithiol. *Macromolecules* **2025**, *58*, 74-86.

(25) Kim, S.; Wittek, K. I.; Lee, Y. Synthesis of poly(disulfide)s with narrow molecular weight distributions via lactone ring-opening polymerization. *Chemical Science* **2020**, *11*, 4882-4886.

(26) Frandsen, M.; El-Chami, K.; Palmfeldt, J.; Melgaard Smidt, J.; Langballe, M. E. T.; Sandahl, A.; Gothelf, K. V. Automated Solid-Phase Oligo(disulfide) Synthesis. *Angewandte Chemie International Edition* **2023**, *62*, e202303170.

(27) Mondal, A.; Kolay, S.; Santra, S.; Sk, S.; Sarkar, S.; Sepay, N.; Molla, M. R. Cascade Initiation of Ring Opening Polymerization for Dynamic Covalent Poly(disulfide)s: One-Step Double Modification and Copoly(disulfide) Synthesis by Living Polymerization. *Macromolecules* **2024**, *57*, 11350-11360.

(28) Penczek, S.; Cypryk, M.; Pretula, J.; Kaluzynski, K.; Lewinski, P. Elemental sulfur and cyclic sulfides. Homo- and copolymerizations. Kinetics, thermodynamics and DFT analysis. *Progress in Polymer Science* **2024**, *152*, 101818.

(29) Zhang, R.; Nie, T.; Fang, Y.; Huang, H.; Wu, J. Poly(disulfide)s: From Synthesis to Drug Delivery. *Biomacromolecules* **2022**, *23*, 1-19.

(30) Kang, K.-S.; Olikagu, C.; Lee, T.; Bao, J.; Molineux, J.; Holmen, L. N.; Martin, K. P.; Kim, K.-J.; Kim, K. H.; Bang, J.; Kumirov, V. K.; Glass, R. S.; Norwood, R. A.; Njardarson, J. T.; Pyun, J. Sulfenyl Chlorides: An Alternative Monomer Feedstock from Elemental Sulfur for Polymer Synthesis. *Journal of the American Chemical Society* **2022**, *144*, 23044-23052.

(31) Lee, T.; Dirlam, P. T.; Njardarson, J. T.; Glass, R. S.; Pyun, J. Polymerizations with Elemental Sulfur: From Petroleum Refining to Polymeric Materials. *Journal of the American Chemical Society* **2022**, *144*, 5-22.

(32) Manjunatha, B. R.; Gallizioli, C.; Fornacon-Wood, C.; Stephan, J.; Stühler, M. R.; Plajer, A. J. Sequence Control in Sulphur-Containing Ring-Opening Co- and Terpolymerisations. *Angewandte Chemie International Edition* **2025**, e202507243.

(33) Lim, J.; Pyun, J.; Char, K. Recent Approaches for the Direct Use of Elemental Sulfur in the Synthesis and Processing of Advanced Materials. *Angewandte Chemie International Edition* **2015**, *54*, 3249-3258.

(34) Yang, H.; Huang, J.; Song, Y.; Yao, H.; Huang, W.; Xue, X.; Jiang, L.; Jiang, Q.; Jiang, B.; Zhang, G. Anionic Hybrid Copolymerization of Sulfur with Acrylate: Strategy for Synthesis of High-Performance Sulfur-Based Polymers. *Journal of the American Chemical Society* **2023**,

145, 14539-14547.

(35) Chung, W. J.; Griebel, J. J.; Kim, E. T.; Yoon, H.; Simmonds, A. G.; Ji, H. J.; Dirlam, P. T.; Glass, R. S.; Wie, J. J.; Nguyen, N. A.; Guralnick, B. W.; Park, J.; Somogyi, Á.; Theato, P.; Mackay, M. E.; Sung, Y.-E.; Char, K.; Pyun, J. The use of elemental sulfur as an alternative feedstock for polymeric materials. *Nature Chemistry* **2013**, *5*, 518.

(36) Gallizioli, C.; Battke, D.; Schlaad, H.; Deglmann, P.; Plajer, A. J. Ring-Opening Terpolymerisation of Elemental Sulfur Waste with Propylene Oxide and Carbon Disulfide via Lithium Catalysis. *Angewandte Chemie International Edition* **2024**, *63*, e202319810.

(37) Deng, Y.; Huang, Z.; Feringa, B. L.; Tian, H.; Zhang, Q.; Qu, D.-H. Converting inorganic sulfur into degradable thermoplastics and adhesives by copolymerization with cyclic disulfides. *Nature Communications* **2024**, *15*, 3855.

(38) Jia, J.; Liu, J.; Wang, Z.-Q.; Liu, T.; Yan, P.; Gong, X.-Q.; Zhao, C.; Chen, L.; Miao, C.; Zhao, W.; Cai, S.; Wang, X.-C.; Cooper, A. I.; Wu, X.; Hasell, T.; Quan, Z.-J. Photoinduced inverse vulcanization. *Nature Chemistry* **2022**, *14*, 1249-1257.

(39) Zhang, J.; Zuo, Y.; Yao, H.; Zhang, J.; Huang, W.; Yang, H.; Zhang, G. Cyclization Polymerization of Elemental Sulfur and Diisocyanate: New Polymerization Toward High-Performance Polymer. *Angewandte Chemie International Edition* **2025**, e202502207.

(40) Zhang, J.; Zang, Q.; Yang, F.; Zhang, H.; Sun, J. Z.; Tang, B. Z. Sulfur Conversion to Multifunctional Poly(O-thiocarbamate)s through Multicomponent Polymerizations of Sulfur, Diols, and Diisocyanides. *Journal of the American Chemical Society* **2021**, *143*, 3944-3950.

(41) Marshall, C. M.; Molineux, J.; Kang, K.-S.; Kumirov, V.; Kim, K.-J.; Norwood, R. A.;

Njardarson, J. T.; Pyun, J. Synthesis of Polycyclic Olefinic Monomers from Norbornadiene for Inverse Vulcanization: Structural and Mechanistic Consequences. *Journal of the American Chemical Society* **2024**, *146*, 24061-24074.

(42) He, L.; Zhao, H.; Theato, P. No Heat, No Light—The Future of Sulfur Polymers Prepared at Room Temperature Is Bright. *Angewandte Chemie International Edition* **2018**, *57*, 13012-13014.

(43) Fan, J.; Ju, C.; Fan, S.; Li, X.; Zhang, Z.; Hadjichristidis, N. Inverse Vulcanization of Aziridines: Enhancing Polysulfides for Superior Mechanical Strength and Adhesive Performance. *Angewandte Chemie International Edition* **2025**, *64*, e202418764.

(44) Huang, H.; Zheng, S.; Luo, J.; Gao, L.; Fang, Y.; Zhang, Z.; Dong, J.; Hadjichristidis, N. Step-growth Polymerization of Aziridines with Elemental Sulfur: Easy Access to Linear Polysulfides and Their Use as Recyclable Adhesives. *Angewandte Chemie International Edition* **2024**, *63*, e202318919.

(45) Tang, H.; Zhang, M.; Zhang, Y.; Luo, P.; Ravelli, D.; Wu, J. Direct Synthesis of Thioesters from Feedstock Chemicals and Elemental Sulfur. *Journal of the American Chemical Society* **2023**, *145*, 5846-5854.

(46) Zheng, B.; Zhong, L.; Wang, X.; Lin, P.; Yang, Z.; Bai, T.; Shen, H.; Zhang, H. Structural evolution during inverse vulcanization. *Nature Communications* **2024**, *15*, 5507.

(47) Tian, T.; Hu, R.; Tang, B. Z. Room Temperature One-Step Conversion from Elemental Sulfur to Functional Polythioureas through Catalyst-Free Multicomponent Polymerizations. *Journal of the American Chemical Society* **2018**, *140*, 6156-6163.

(48) Cao, W.; Dai, F.; Hu, R.; Tang, B. Z. Economic Sulfur Conversion to Functional

Polythioamides through Catalyst-Free Multicomponent Polymerizations of Sulfur, Acids, and Amines. *Journal of the American Chemical Society* **2020**, *142*, 978-986.

(49) Huang, Y.; Yu, Y.; Hu, R.; Tang, B. Z. Multicomponent Polymerizations of Elemental Sulfur, CH_2Cl_2, and Aromatic Amines toward Chemically Recyclable Functional Aromatic Polythioureas. *Journal of the American Chemical Society* **2024**, *146*, 14685-14696.

(50) Chao, J.-Y.; Yue, T.-J.; Ren, B.-H.; Gu, G.-G.; Lu, X.-B.; Ren, W.-M. Controlled Disassembly of Elemental Sulfur: An Approach to the Precise Synthesis of Polydisulfides. *Angewandte Chemie International Edition* **2022**, *61*, e202115950.

(51) Ottou, W. N.; Sardon, H.; Mecerreyes, D.; Vignolle, J.; Taton, D. Update and challenges in organo-mediated polymerization reactions. *Progress in Polymer Science* **2016**, *56*, 64-115.

(52) Nair, D. P.; Podgórski, M.; Chatani, S.; Gong, T.; Xi, W.; Fenoli, C. R.; Bowman, C. N. The Thiol-Michael Addition Click Reaction: A Powerful and Widely Used Tool in Materials Chemistry. *Chemistry of Materials* **2014**, *26*, 724-744.

(53) Yang, H.; Zhang, J.; Huang, W.; Zhang, G. Transforming Element Sulfur to High Performance Closed-Loop Recyclable Polymer via Proton Transfer Enabled Anionic Hybrid Copolymerization. *Angewandte Chemie International Edition* **2025**, *64*, e202414244.

(54) Bao, J.; Martin, K. P.; Cho, E.; Kang, K.-S.; Glass, R. S.; Coropceanu, V.; Bredas, J.-L.; Parker, W. O. N., Jr.; Njardarson, J. T.; Pyun, J. On the Mechanism of the Inverse Vulcanization of Elemental Sulfur: Structural Characterization of Poly(sulfur-random-(1,3-diisopropenylbenzene)). *Journal of the American Chemical Society* **2023**, *145*, 12386-12397.

(55) Wu, Z.; Pratt, D. A. Radical Substitution Provides a Unique Route to Disulfides. *Journal*

of the American Chemical Society **2020**, *142*, 10284-10290.

(56) Zhang, Q.; Li, Y.; Zhang, L.; Luo, S. Catalytic Asymmetric Disulfuration by a Chiral Bulky Three-Component Lewis Acid-Base. *Angewandte Chemie International Edition* **2021**, *60*, 10971-10976.

(57) Zhou, F.; He, X.; Zhou, M.; Li, N.; Wang, Q.; Zhang, X.; Lian, Z. Generation of perthiyl radicals for the synthesis of unsymmetric disulfides. *Nature Communications* **2025**, *16*, 23.

(58) Huang, P.; Wang, P.; Tang, S.; Fu, Z.; Lei, A. Electro-Oxidative S−H/S−H Cross-Coupling with Hydrogen Evolution: Facile Access to Unsymmetrical Disulfides. *Angewandte Chemie International Edition* **2018**, *57*, 8115-8119.

(59) Jin, S.; Li, S.-J.; Ma, X.; Su, J.; Chen, H.; Lan, Y.; Song, Q. Elemental-Sulfur-Enabled Divergent Synthesis of Disulfides, Diselenides, and Polythiophenes from β-CF_3-1,3-Enynes. *Angewandte Chemie International Edition* **2021**, *60*, 881-888.

(60) Ong, C. L.; Titinchi, S.; Juan, J. C.; Khaligh, N. G. An Overview of Recent Advances in the Synthesis of Organic Unsymmetrical Disulfides. *Helvetica Chimica Acta* **2021**, *104*, e2100053.

(61) Schmitt, C. W.; Dodd, L. J.; Walz, J. K.; Deterding, L.; Lott, P.; Grimm, A. P.; Shaver, M. P.; Hasell, T.; Théato, P. A critical review on the sustainability of inverse vulcanised polymers. *RSC Sustainability* **2025**, *3*, 4190-4227.

(62) Tveryanovich, Y. S.; Pankin, D. V.; Sukhanov, M. V.; Churbanov, M. F. Isotope effect in Raman scattering spectra of $^{32}S_8$–$^{34}S_8$ solid mixtures. *Optik* **2021**, *240*, 166861.

(63) Duarte, M. E.; Huber, B.; Theato, P.; Mutlu, H. The unrevealed potential of elemental sulfur for the synthesis of high sulfur content bio-based aliphatic polyesters. *Polymer Chemistry*

2020, *11*, 241-248.

Acknowledgment

We gratefully acknowledge the financial support of the National Natural Science Foundation of China (52373014, received by Chengjian Zhang).

Author contributions

Yue Sun carried out most of experiments and wrote the draft. Yuxiang Cao carried out the analysis of polymer structure. Xiong Liu carried out the analysis of polymerization mechanism. Chengjian Zhang conceived, designed, and directed the investigation and revised the manuscript. Xinghong Zhang directed the investigation and revised the manuscript.

Competing interests

The authors declare no competing interests.

Figure legends

Figure 1. Synthesis of disulfide-containing polymers. (a) Traditional approaches to poly(disulfide)s rely on oxidative coupling of dithiols or ROP of cyclic disulfides. (b) The inverse vulcanization to yield crosslinked poly(sulfide)s. (c) This work developed the step-growth addition polymerization to synthesize poly(ester disulfide)s from S_8, dithiols, and diacrylates.

Figure 2. Synthesis and NMR analysis (in $CDCl_3$) of disulfides. (a) The addition reaction of *n*-

hexylthiol, S_8, and methylacrylate. (b) ^{1}H NMR (400 MHz) and (c) ^{13}C NMR (101 MHz) spectra of the mixed crude products. (d) ^{1}H NMR and (e) ^{13}C NMR spectra of purified **A1** (middle), **A2** (up), and **A3** (down). (f) Partially enlarged ^{1}H NMR and (g) ^{13}C NMR spectra of purified **A1** (up) and the mixed crude products (down).

Figure 3. DFT calculations to investigate the three-component coupling reaction mechanism. (a) Free energies associated with the proposed mechanism of the formation of asymmetric disulfides. (b, c) Free energies associated with the formation of symmetrical disulfide through thiol/disulfide exchange reaction.

Figure 4. Synthesis of **P1–P6** using S_8, dithiols, and diacrylates/diamides. Polymerization conditions: at room temperature for 2 h, $[S]_0$:[dithiol]$_0$:[diacrylate]$_0$:[MTBD]:[PPNCl] = 400:200:200:1:1. M_n and $Đ$ values are determined by GPC in THF, calibrated with polystyrene standards.

Figure 5. Structure analysis of **P1**. (a) ^{1}H NMR (400 MHz) and (b) ^{13}C NMR spectra (101 MHz, in $CDCl_3$) of **P1**. (c) Raman spectrum of **P1**. (d) MALDI-TOF MS of low-M_n **P1**, *n* for alkyl disulfide units, *m* for ester-containing disulfide units.

Figure 6. Thermal, mechanical, and degradation properties of the obtained polymers. (a) TGA curves. (b) DSC curves obtained from the second scan. (c) Tensile stress-strain curves. (d) Cyclic tensile testing without delay of **P5**. (e) Cyclic tensile testing without delay of **P4**. (f) GPC curves of **P2** varying during reduction degradation.

Editorial Summary:

The synthesis of high molecular weight poly(disulfide)s typically requires harsh conditions or the complex cyclic disulfide monomers. Here, the authors report a mild, room-temperature multicomponent polymerisation using elemental sulfur to yield high molecular weight poly(ester disulfide)s

Peer review information: *Nature Communications* thanks Hatice Mutlu, Alex Plajer, and the other, anonymous, reviewer(s) for their contribution to the peer review of this work. A peer review file is available.

(a) Previous methods for the synthesis of poly(disulfide)s

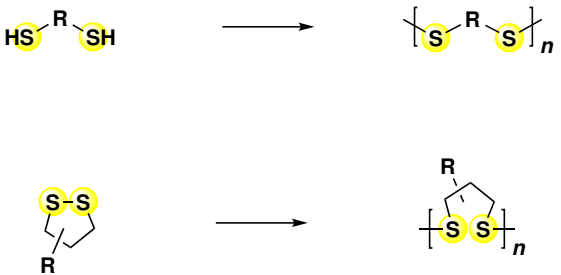

Disulfide-containing Monomers

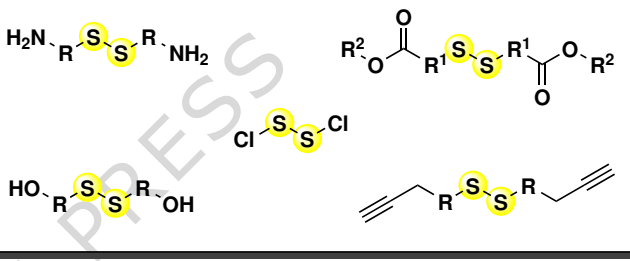

(b) Inverse vulcanization to yield crosslinked poly(sulfide)s

(c) This work: Synthesis of poly(ester disulfide)s from dithiols, diacrylates, and S_8

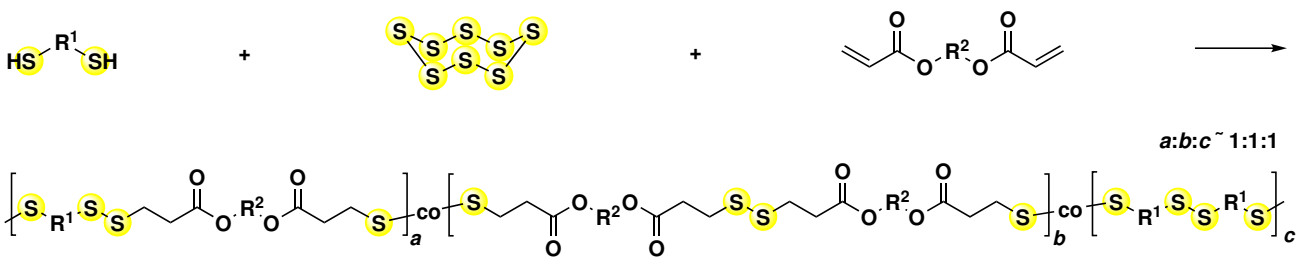

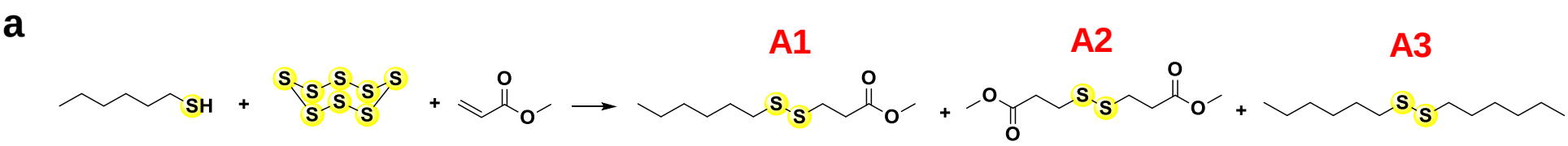
a
A1
A2
A3
SH

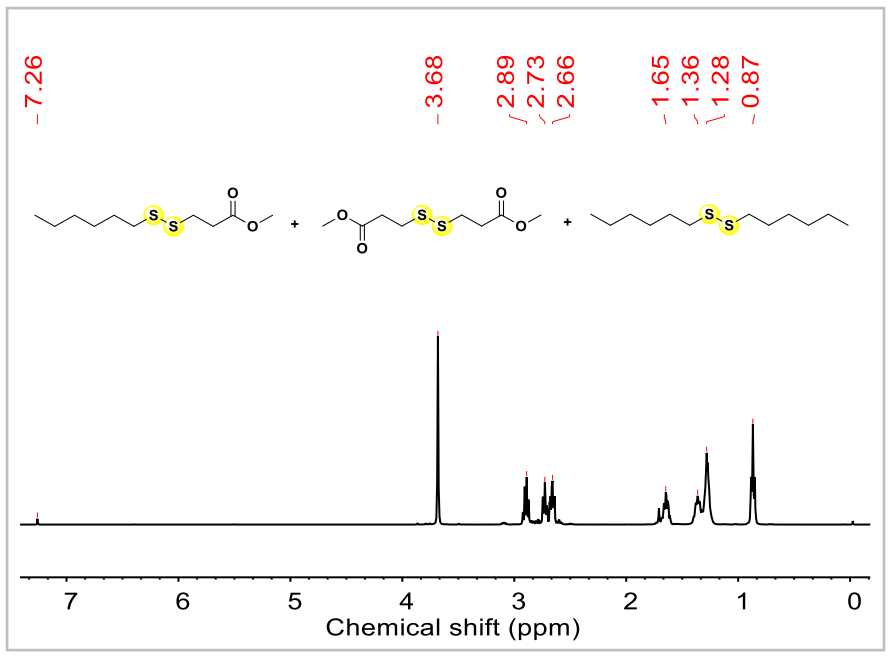
b
7.26
3.68
2.89
2.73
2.66
1.65
1.36
1.28
0.87
Chemical shift (ppm)

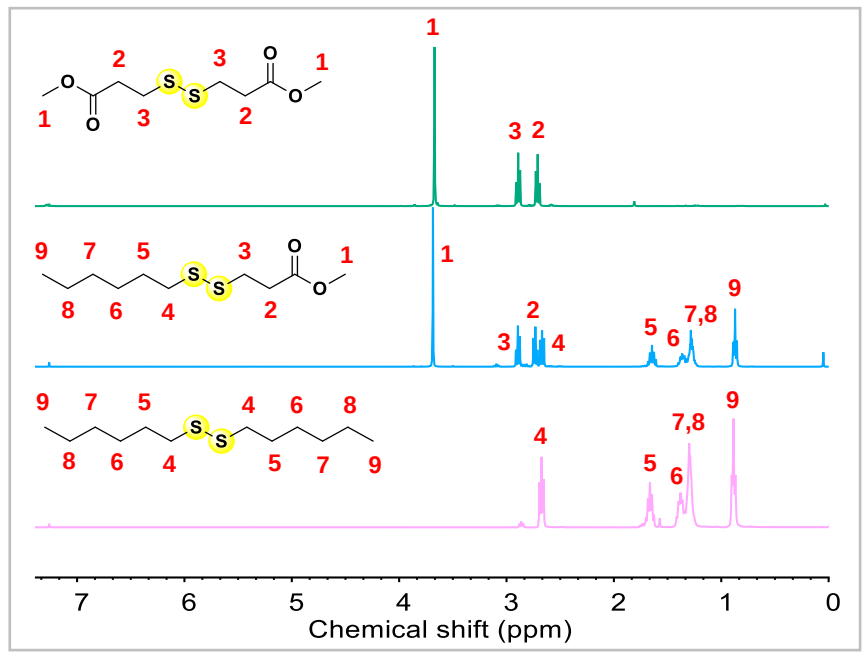
d
Chemical shift (ppm)

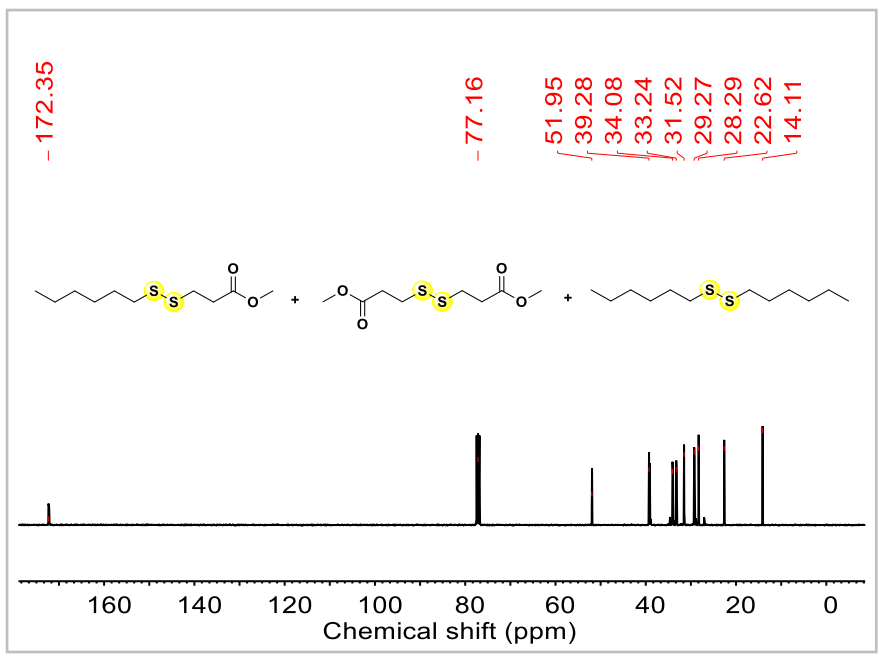
c
172.35
77.16
51.95
39.28
34.08
33.24
31.52
29.27
28.29
22.62
14.11
Chemical shift (ppm)

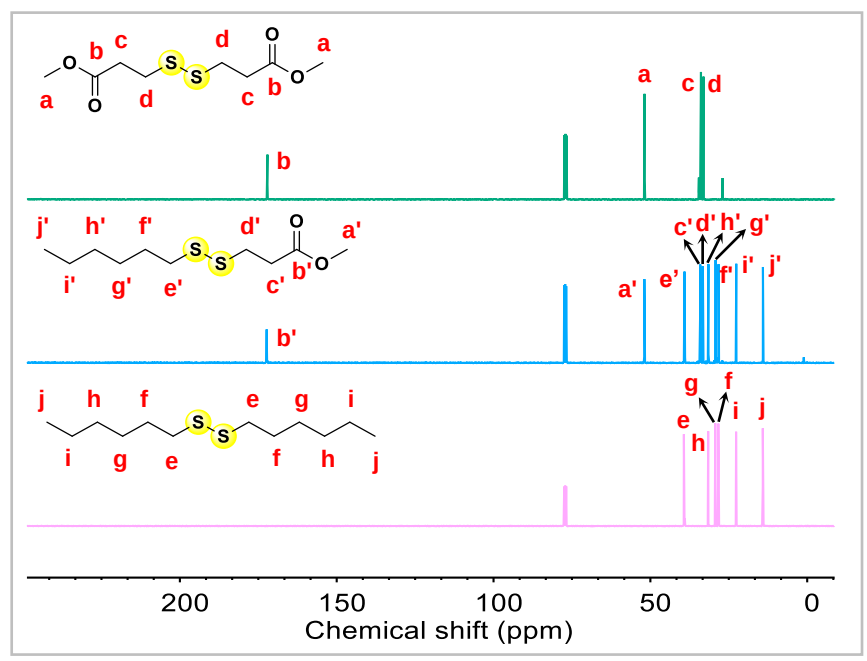
e
Chemical shift (ppm)

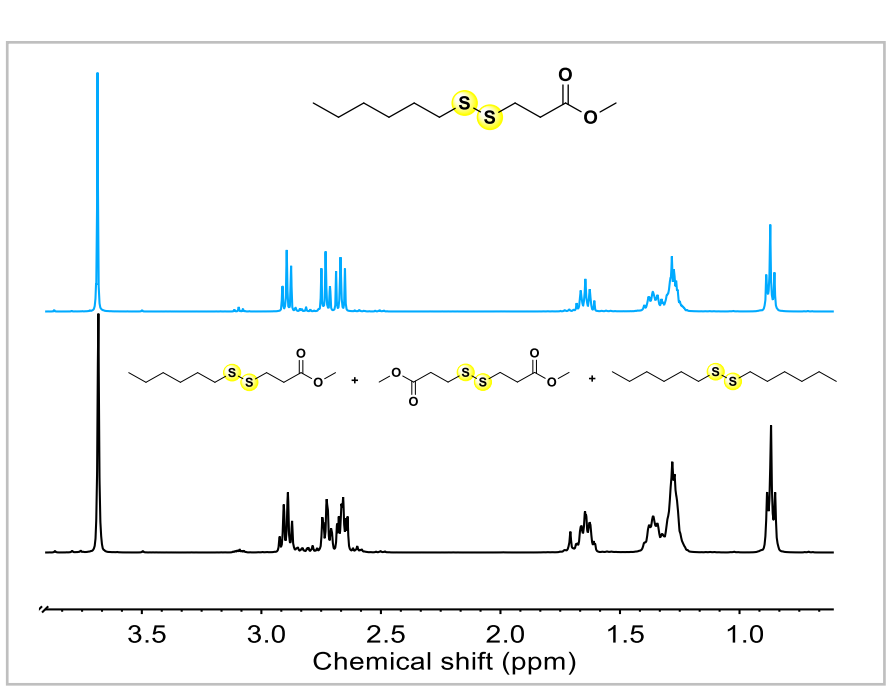
f
Chemical shift (ppm)

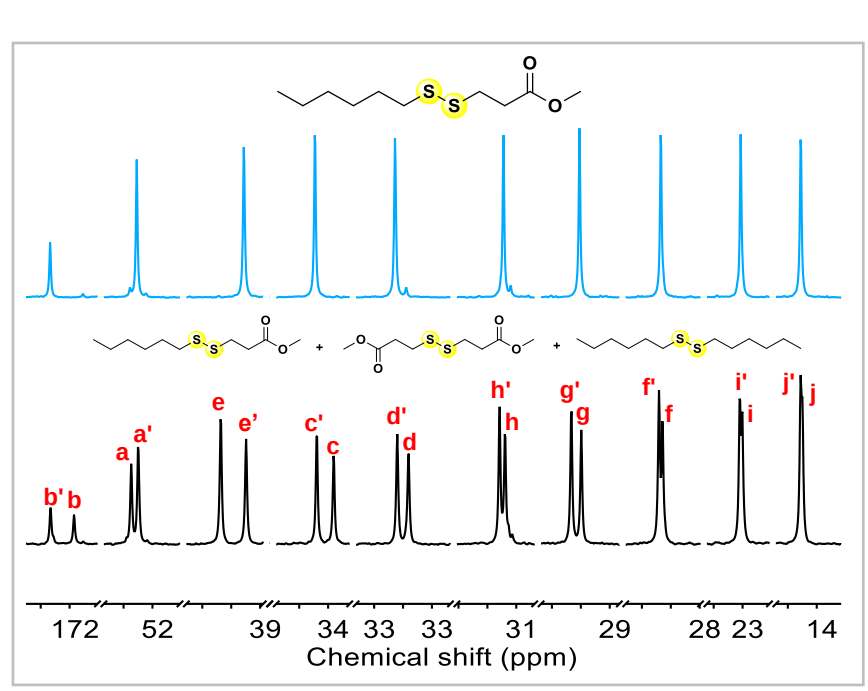
g
Chemical shift (ppm)

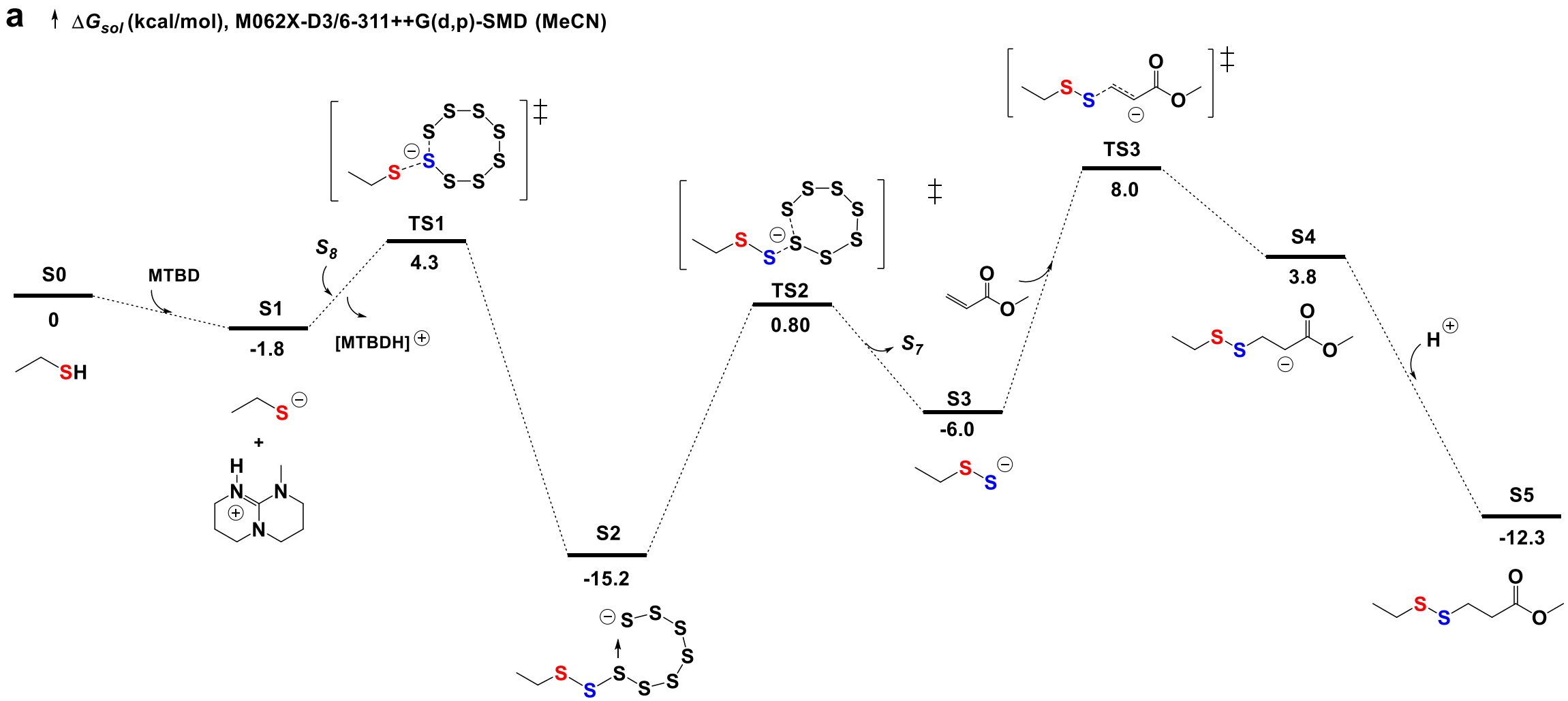

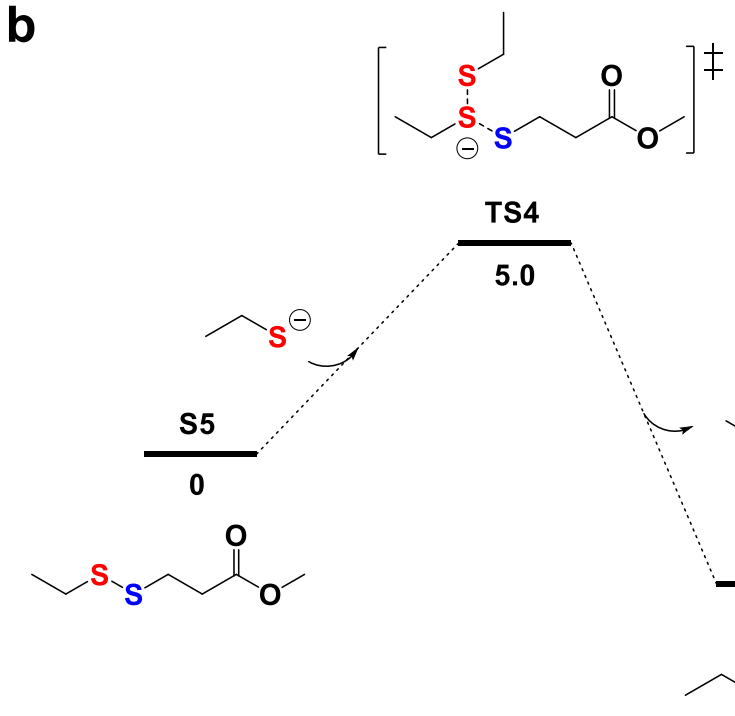

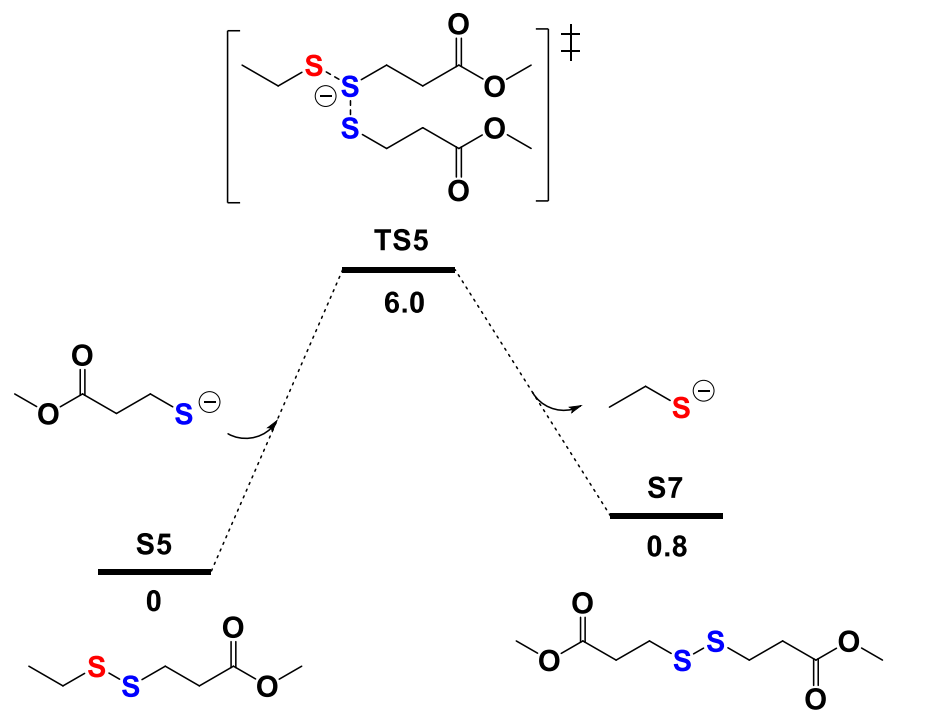

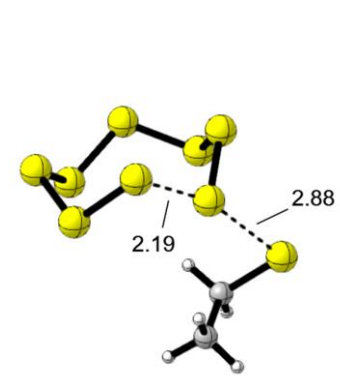

TS1

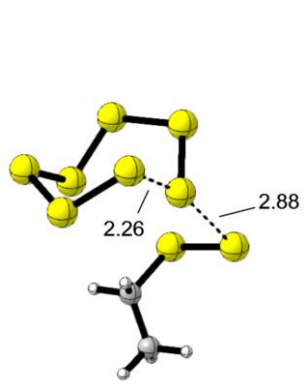

TS2

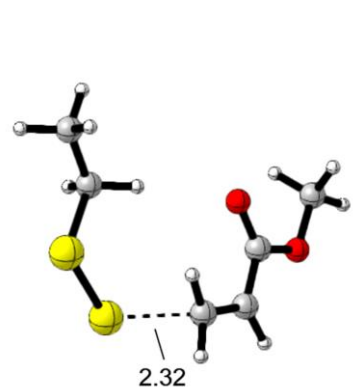

TS3

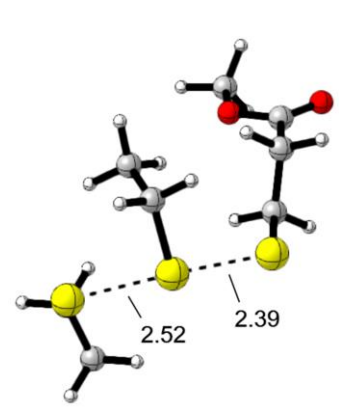

TS4

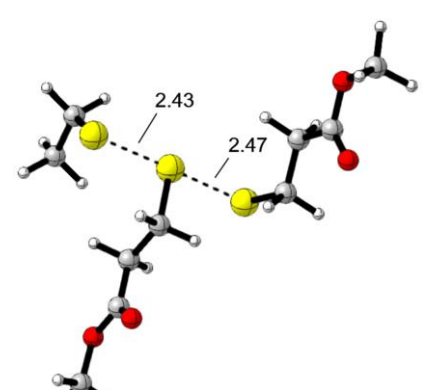

TS5

M1

M2

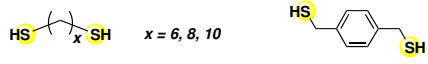

M3

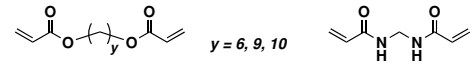

a:*b*:*c* ~ 1:1:1

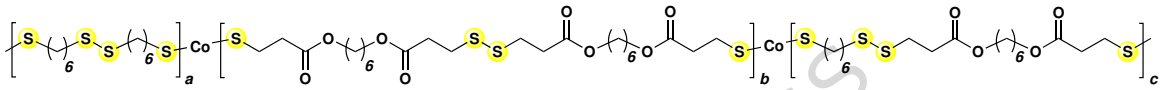

P1, 22.1 kDa (2.0)

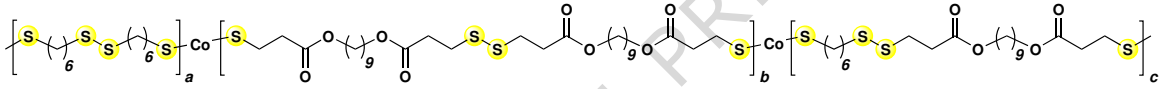

P2, 20.8 kDa (2.6)

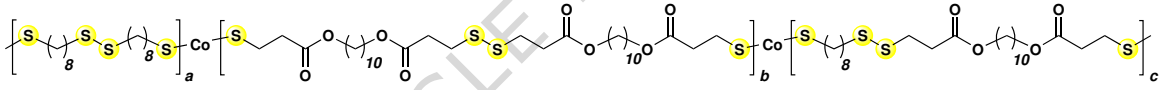

P3, 21.3 kDa (1.8)

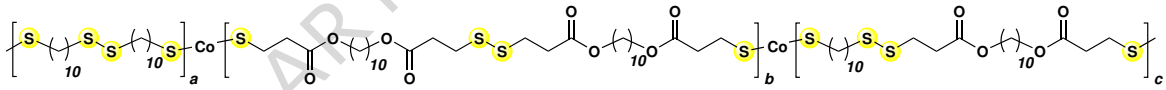

P4, 42.0 kDa (2.1)

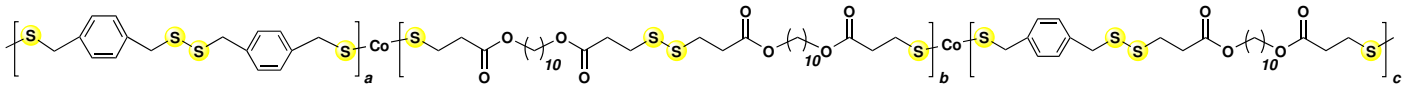

P5, 27.7 kDa (1.4)

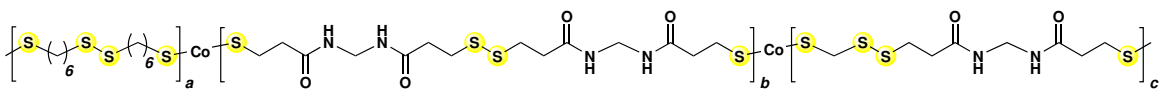

P6, M_n not determined due to low solubility in THF

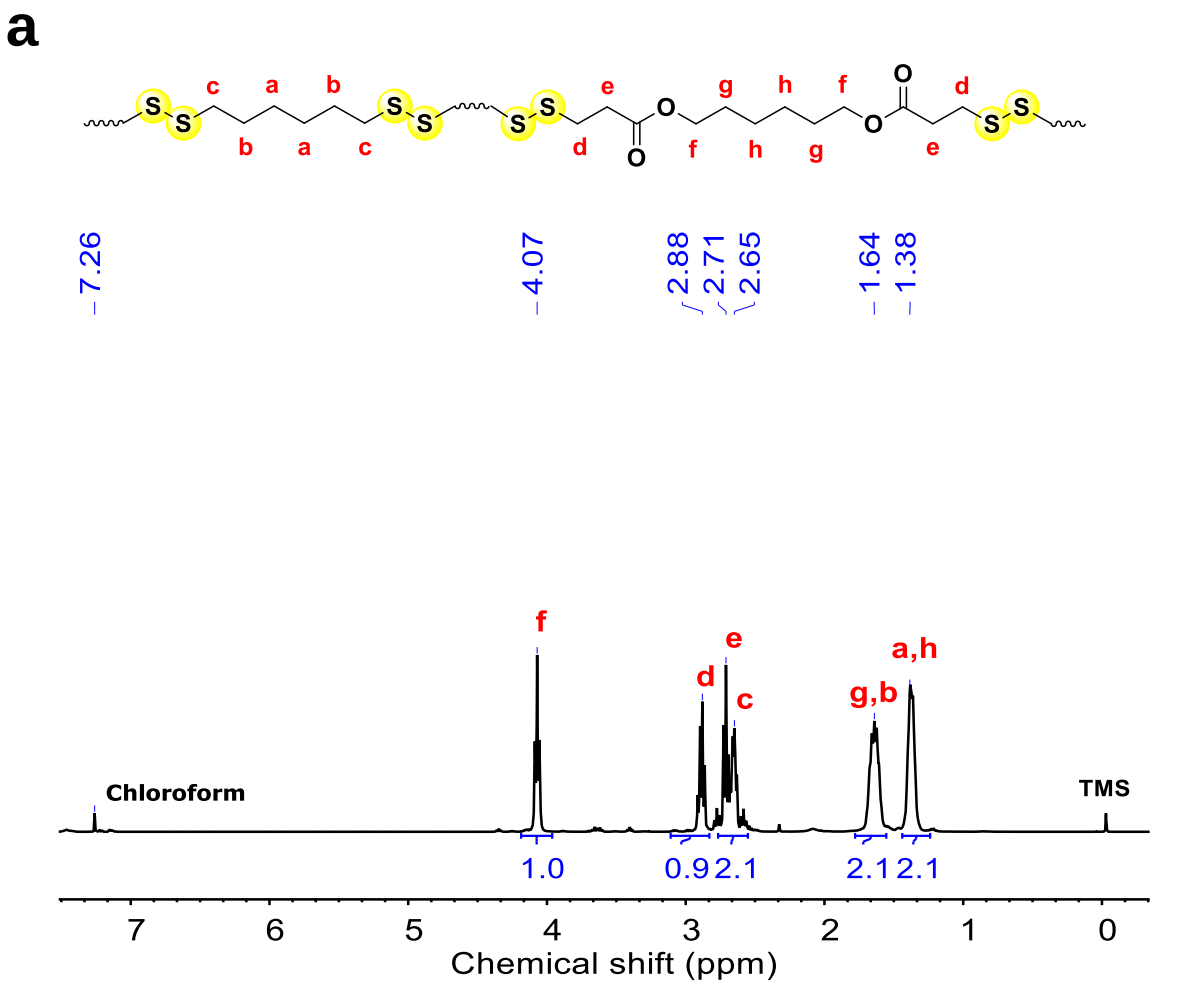
a
7.26
4.07
2.88
2.71
2.65
1.64
1.38
f
e
d
c
g,b
a,h
Chloroform
TMS
1.0
0.92.1
2.12.1
Chemical shift (ppm)

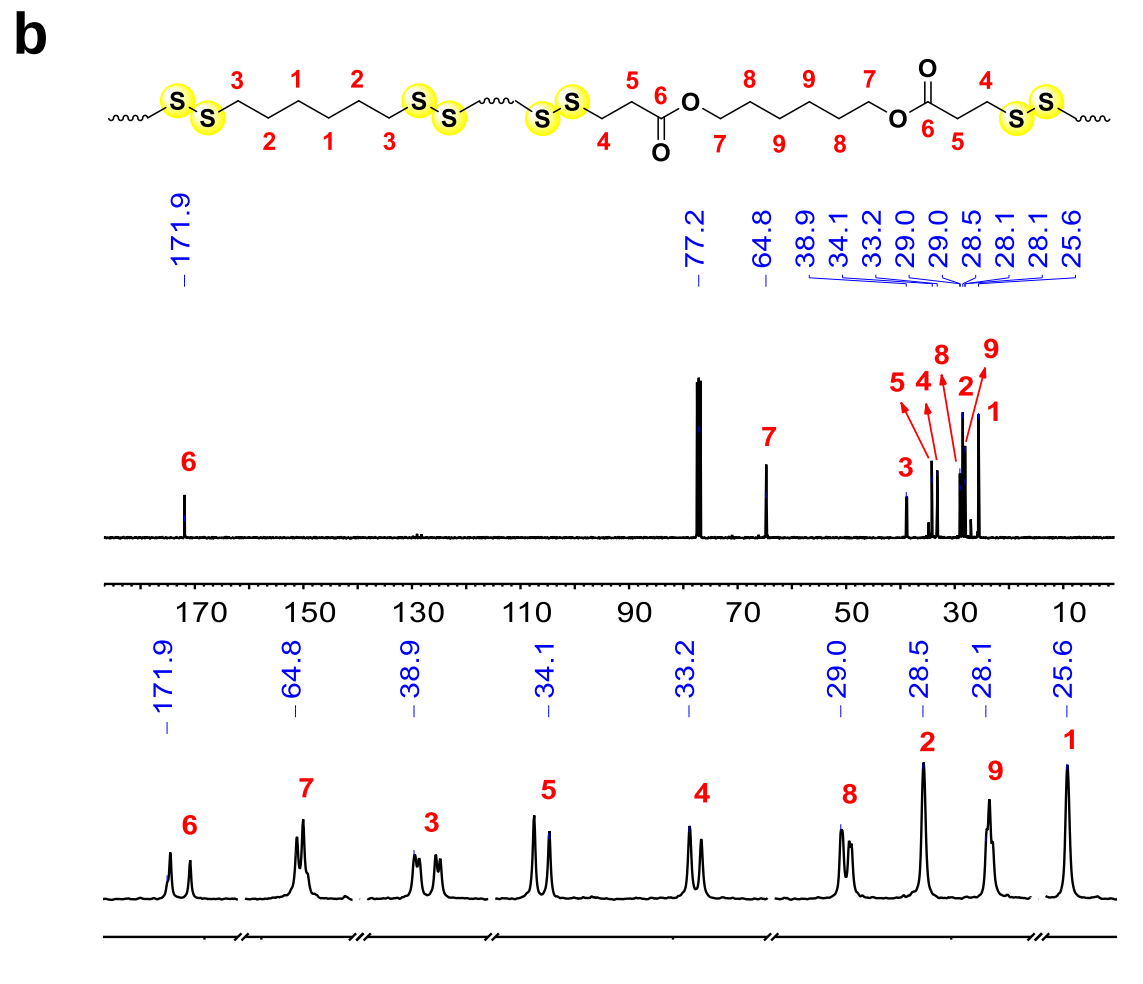
b
171.9
77.2
64.8
38.9
34.1
33.2
29.0
29.0
28.5
28.1
28.1
25.6
Chemical shift (ppm)

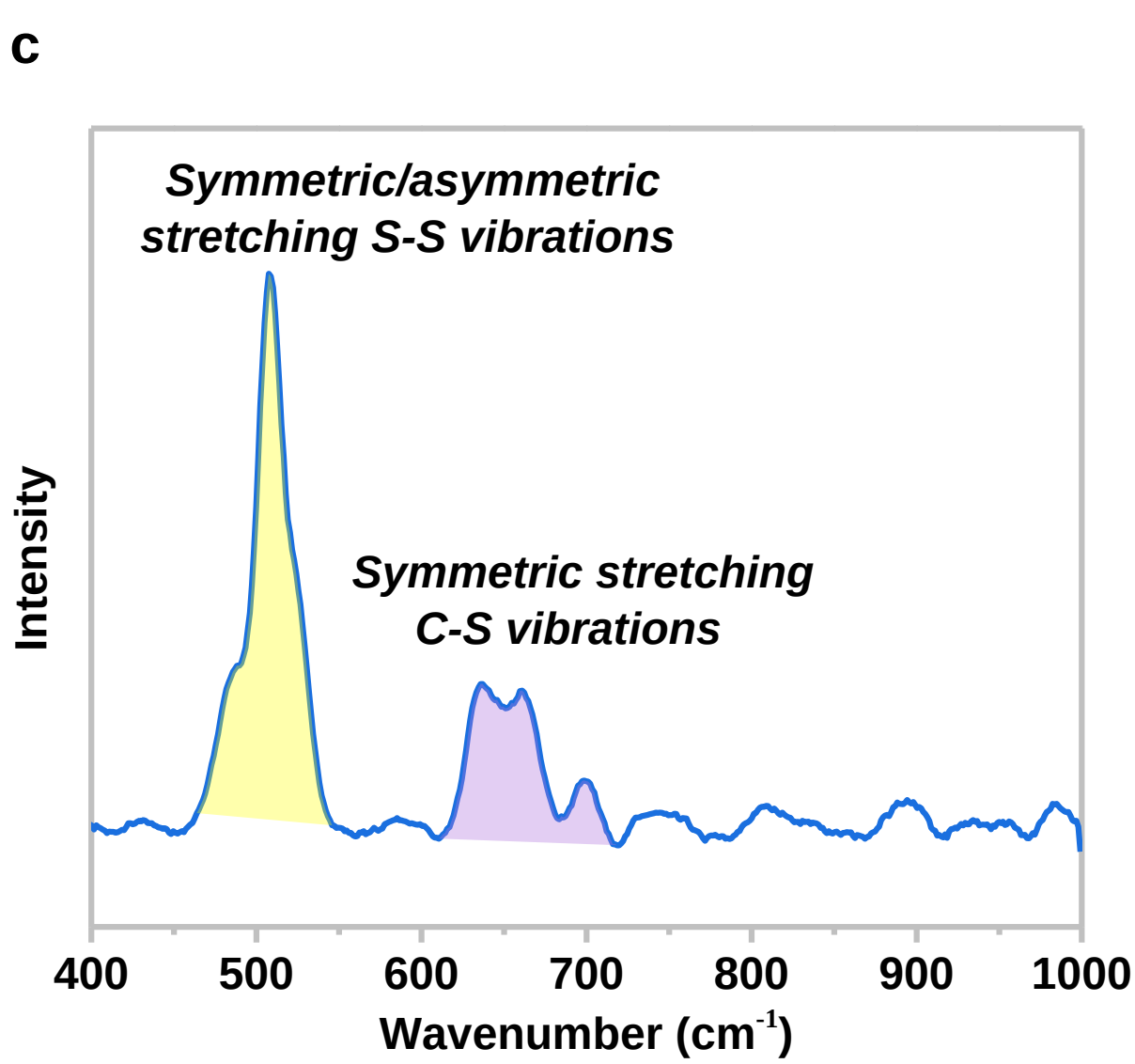
c
Symmetric/asymmetric
stretching S-S vibrations
Symmetric stretching
C-S vibrations
Intensity
Wavenumber (cm-1)

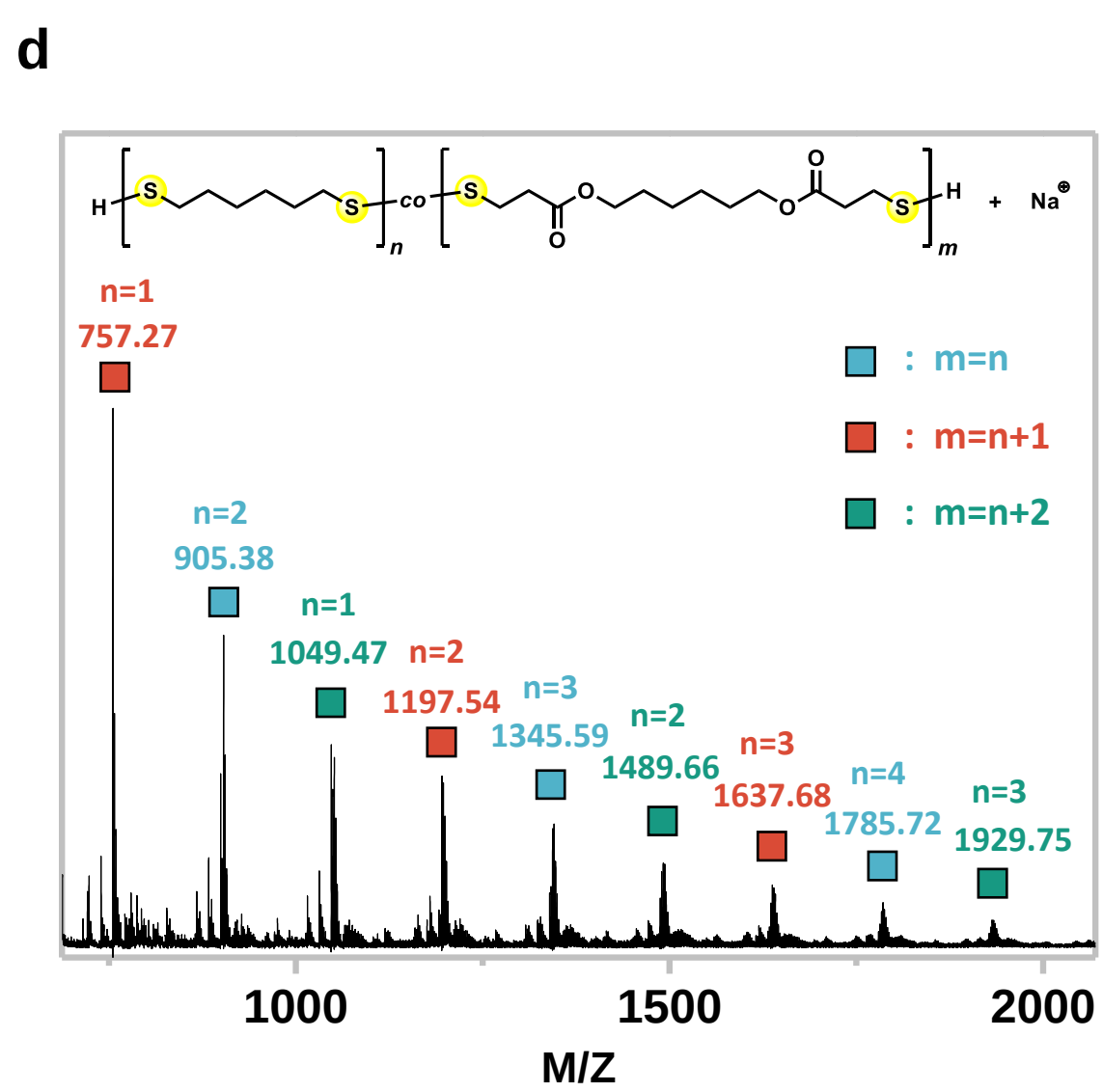
d
n=1
757.27
n=2
905.38
n=1
1049.47
n=2
1197.54
n=3
1345.59
n=2
1489.66
n=3
1637.68
n=4
1785.72
n=3
1929.75
: m=n
: m=n+1
: m=n+2
M/Z

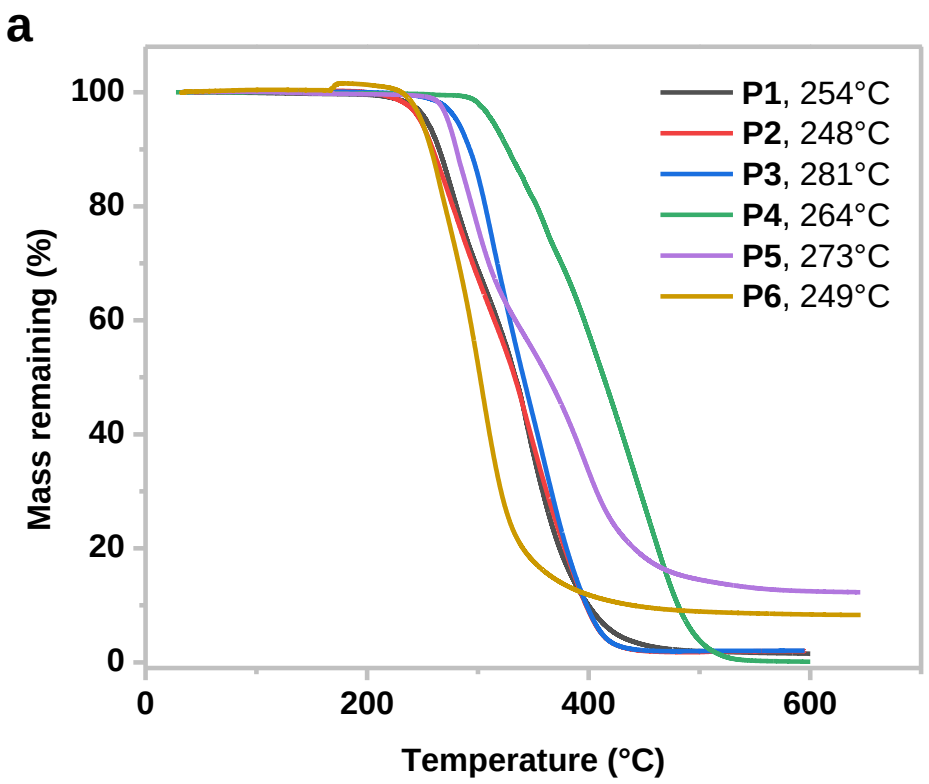
a
Mass remaining (%)
Temperature (°C)
P1, 254°C
P2, 248°C
P3, 281°C
P4, 264°C
P5, 273°C
P6, 249°C

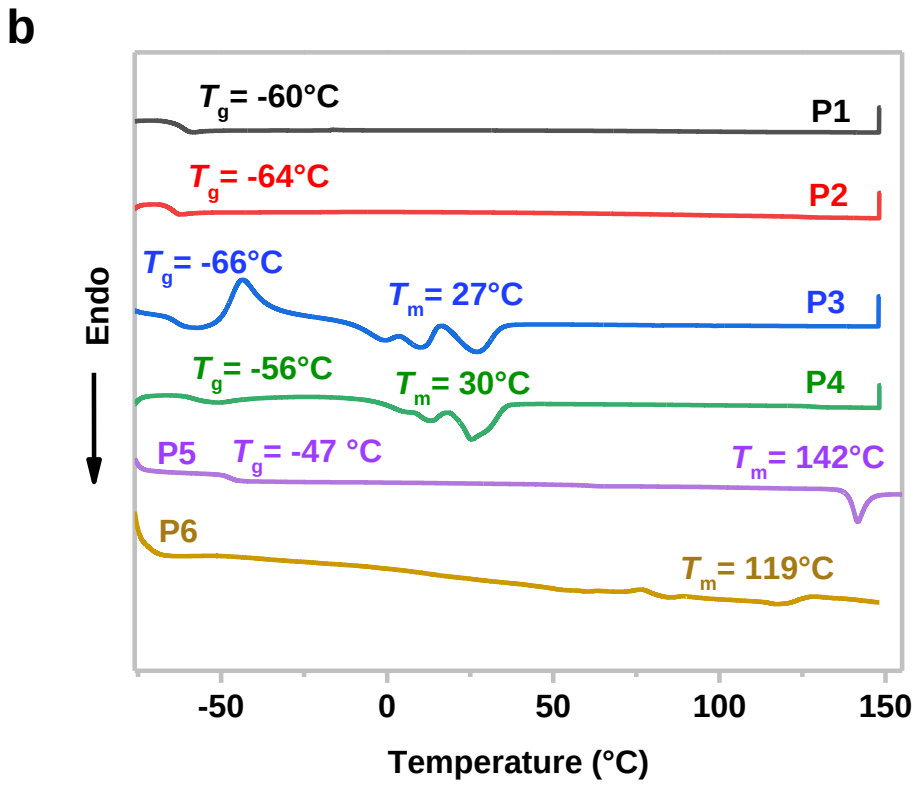
b
Endo
Temperature (°C)
Tg= -60°C
P1
Tg= -64°C
P2
Tg= -66°C
Tm= 27°C
P3
Tg= -56°C
Tm= 30°C
P4
P5
Tg= -47 °C
Tm= 142°C
P6
Tm= 119°C

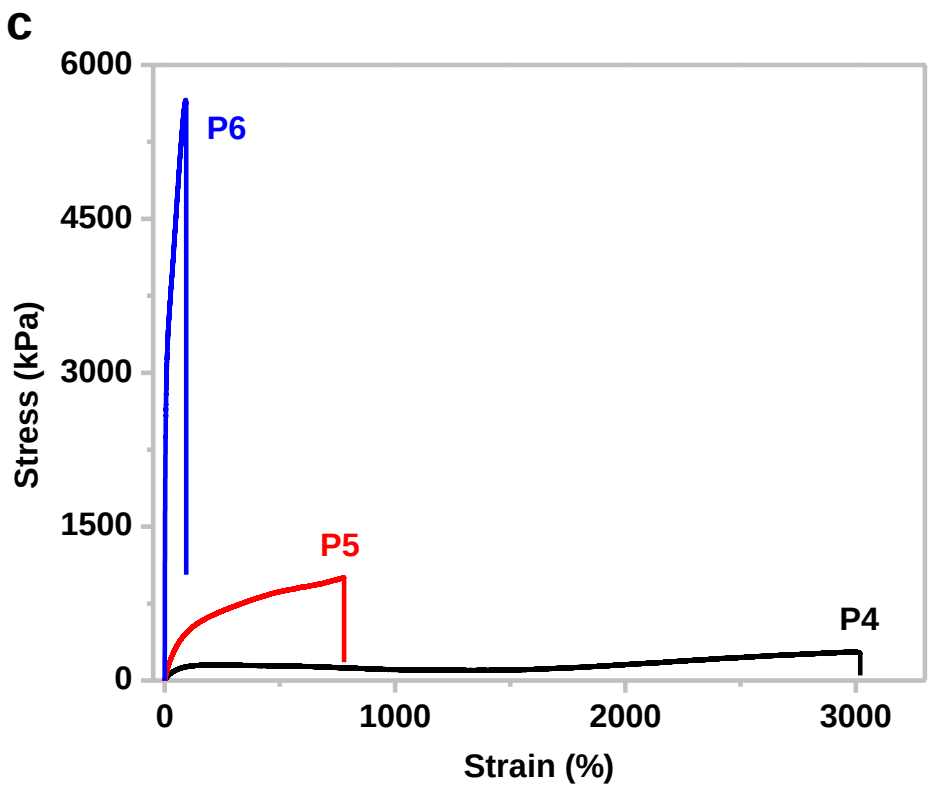
c
Stress (kPa)
Strain (%)
P6
P5
P4

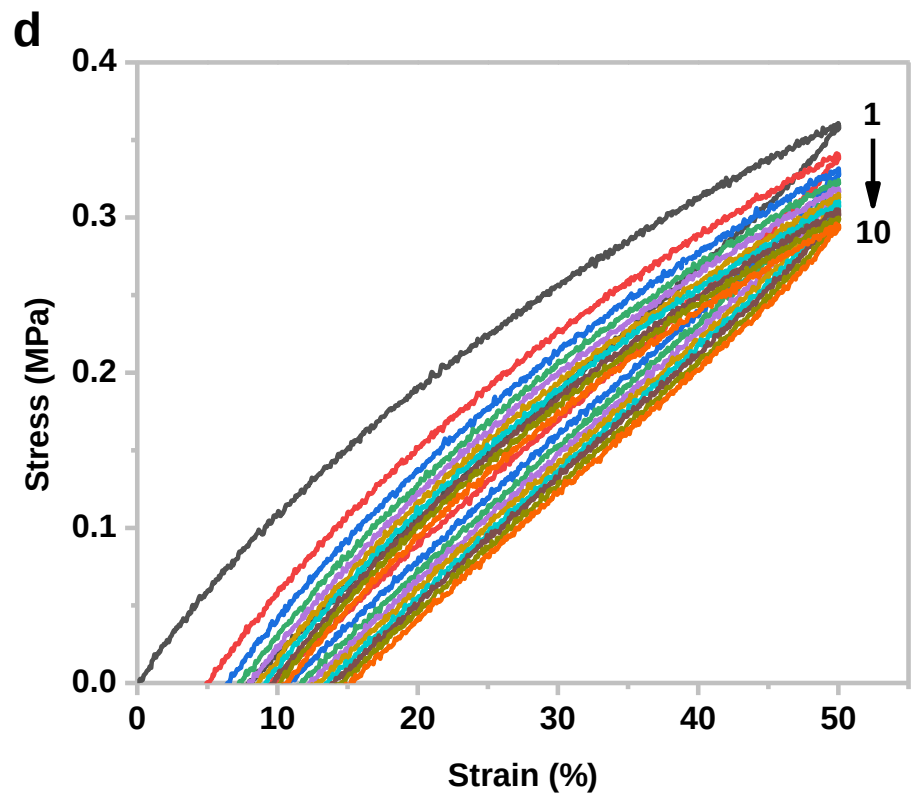
d
Stress (MPa)
Strain (%)
1
10

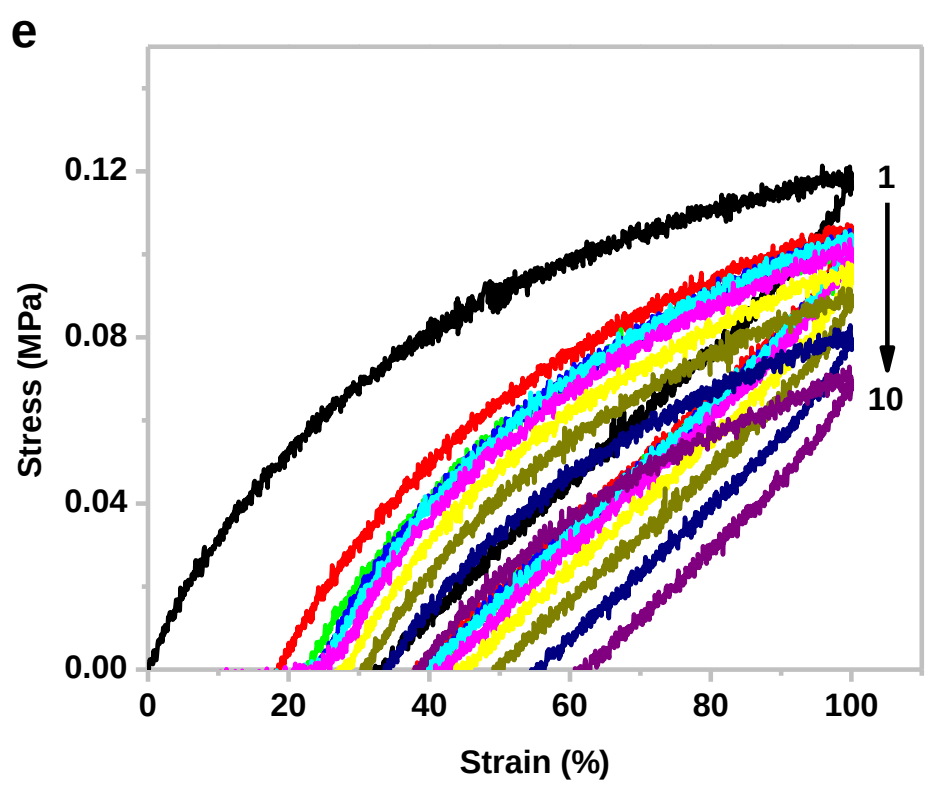
e
Stress (MPa)
Strain (%)
1
10

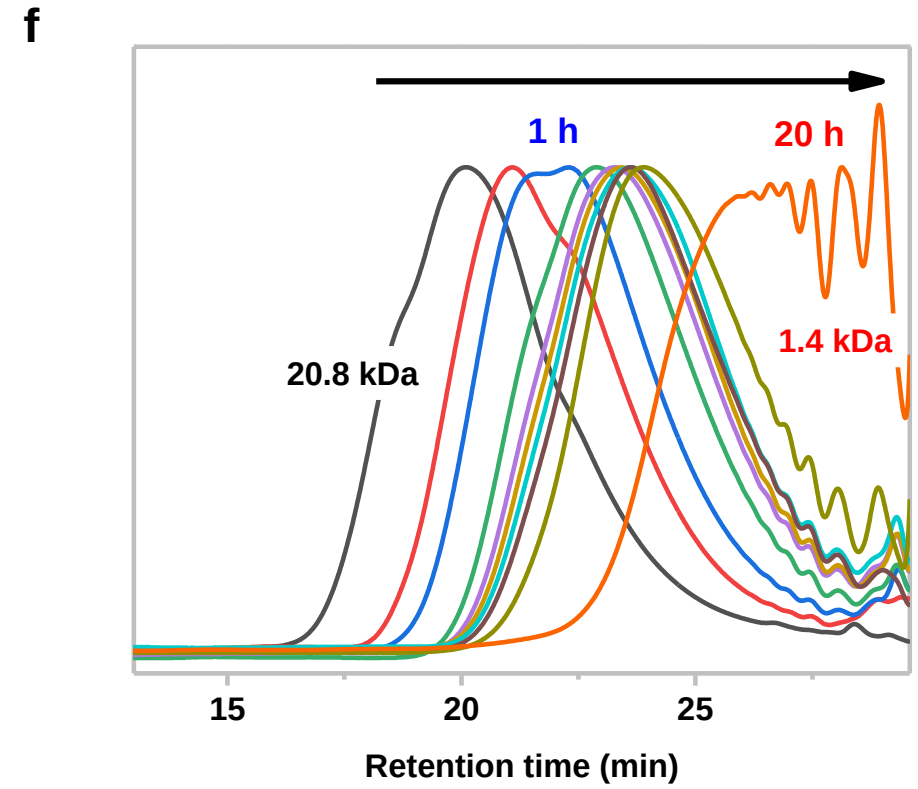
f
1 h
20 h
20.8 kDa
1.4 kDa
Retention time (min)